Development and comparative lifecycle assessment of various LDPE and HDPE
production processes based on CO_2 capture and utilization

Farah Mufarrij

A Thesis

in

the Department

of

Chemical and Materials Engineering

Presented in Partial Fulfillment of the Requirements

For the Degree of Master of Applied Science at

Concordia University

Montreal, Quebec, Canada

August 2022

This is to certify that the thesis prepared

By: Farah Mufarrij

Entitled: Development and comparative lifecycle assessment of various LDPE

and HDPE production processes based on CO_2 capture and utilization

and submitted in partial fulfillment of the requirements for the degree of

Master of Applied Science (Chemical and Materials Engineering)

complied with the regulations of the University and meets the accepted standards with respect to originality and quality.

Signed by the final Examining Committee:

_____Chair
    Dr. Melanie Hazlett

_____Examiner
    Dr. Ivan Kantor

_____Supervisor
    Dr. Yaser Khojasteh

Approved by _____
    Dr. Zhibin Ye, Graduate Program Director

August 2022 _____
    Dr. Mourad Debbabi, Dean Gina Cody School of Engineering
    and Computer Science

ABSTRACT

Development and comparative lifecycle assessment of various LDPE and HDPE

production processes based on CO_2 capture and utilization

Farah Mufarrij

Low-density polyethylene (LDPE) and high-density polyethylene (HDPE) are some of the most commonly used materials worldwide. These polymers are typically produced through the polymerization of ethylene which is conventionally produced through the energy-intensive steam cracking of naphtha or ethane. However, the conventional production process for LDPE and HDPE results in significant greenhouse gas emissions (1.92 and 1.86 kg CO_2/kg of polymer, respectively).

Hence, this work focuses on the design of alternative pathways based on CO_2 capture and utilization (CCU) for polymer production. The proposed pathways for CCU-polymers are based on the conversion of CO_2 to methanol, followed by the methanol-to-olefins (MTO) process to produce mainly ethylene, and consequently LDPE and HDPE from ethylene. The process design and simulation of the entire pathway are conducted in AspenPlus, while the life cycle assessment (LCA) is done through OpenLCA.

The LCA results showed that the CCU-MTO pathway is an environmentally attractive option, particularly in regions where renewable (low-carbon) electricity is more prominent, such as Quebec and Ontario, where negative CO_2 emissions are achieved. This makes polymer production via the proposed method suitable for the permanent mitigation of CO_2.

Acknowledgments

First, I would like to thank and express my sincere gratitude to my supervisor Dr. Yaser Khojasteh for his support, patience, and immense knowledge. He guided me through the whole research and writing process. I could not imagine a better mentor for my master's thesis. I would like to thank the team at National Resources Canada (NRCan) for their help and input regarding my results.

My thanks also goes to the examining committee, and to my teammates who listened to my challenges during team meetings. I would also like to extend thanks to my partner, Nassif who was by my side through this whole process. As well as my friends for their encouragements.

Last but not least, I would like to thank my family, Raif, Julie, Reem, Nadine, and Dana, for always being there for me and for their unconditional love.

Table of Contents

List of Figures

List of Tables

1. Introduction

Climate change is proven to be a phenomenon matter of growing concern. It is defined as the variations in weather patterns due to greenhouse gas (GHG) emissions [1]. The role of GHGs is to absorb and release heat progressively over time [2]. Without this action, the average global temperature would have been less by about 33°C [2,3]. However, the increase in GHGs disrupted the Earth's energy balance, such that more heat is being absorbed than released, elevating the global average temperature [2]. The world is exhibiting elevated global temperatures that are not only increasing the negative impact of natural disasters, such as flash floods, storms, drought, and consequently water shortages, but also endangering the lives of humans and other living things [4]. Other impacts of GHG emissions include extreme weather conditions, degradation of the ozone layer, and land degradation [5].

A report by the Intergovernmental Panel on Climate Change (IPCC) in 2018 indicated that the global average temperature has increased by 1°C since 1900 [6]. The Paris Agreement, established in 2015, mentioned that in order to reduce the impacts of climate change, there should be a global effort to maintain global warming temperatures realistically below 2°C (ideally below 1.5°C) above pre-industrial temperatures [7]. If the global temperature is to be limited to 2°C above pre-industrial levels by 2030, the greenhouse gas emissions should decrease by 30%, as mentioned in a report by the United Nations Environment Programme [8]. Additionally, if the limit of global temperature is to be set at 1.5°C above pre-industrial temperatures, then GHG emissions must be reduced by 55% by 2030 [8].

In order to create an appropriate plan to address the climate crisis, it is important to know the origin of the GHGs. GHGs are both naturally-occurring and man-made, with the exception of halocarbons, which are only man-made [9]. Carbon dioxide (CO_2), methane (CH_4), and nitrous oxide (N_2O) are all part of the Earth's cycle [9]. This implies that a natural balance exists among these greenhouse gases. Compared to CO_2, the most prevalent GHG, more heat is absorbed by other GHGs, such as CH_4 and N_2O [2]. However, CO_2 alone contributed to the disruption of two-thirds of the global energy balance, making it the most significant [2]. Since the rate at which these natural GHG emissions occur is too slow to solely justify the rapid rate at which global warming has been increasing over the past few decades, then it is with high confidence that the disruption the equilibrium in the Earth's climate is attributed to anthropogenic actions, mainly fossil fuel (oil, gas, and coal) burning [4,10–12].

The world witnessed a record decline in CO_2 emissions in 2020, a direct result of the COVID-19 pandemic [8]. The emissions coming from fossil fuel burning and industrial activities decreased by 5.4% [8,13]. However, after the vaccine roll-out, the economy recovered and CO_2 emissions grew once again; 36.3 billion tonnes of CO_2 were released in 2021, a 6% increase from 2020 as can be seen by Figure 1-1[13].
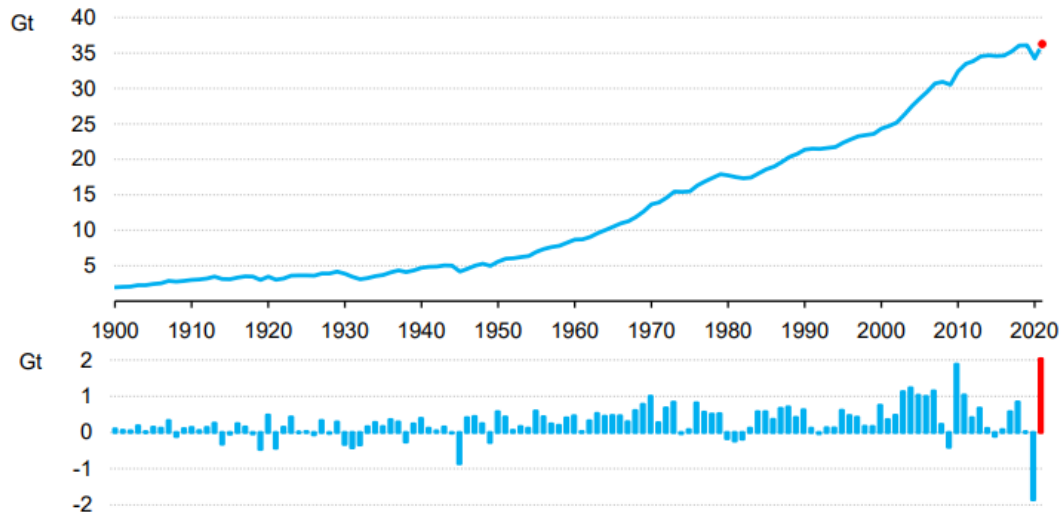
Figure 1-1: Total energy- and industry- related CO_2 emissions from 1900 to 2021 and the respective annual change [13]

The rebound of the economy after the pandemic, countered the decrease of emissions, so much so that 2021 emissions are 180 megatonnes greater than 2019 emissions, which is the highest year-on year growth since 2010 [13]. This aligns with the estimates released in a report by the International Energy Agency [14].

According to Our World in Data, 84.3% of global energy is sourced from fossil fuels, making them the main source of energy [15]. In 2020, the industrial sector accounted for 21% of global CO_2 emissions, such that it is only exceeded by electricity and heat production, or the power sector (37%) [16]. The largest contributors to GHG in the industry sector include cement, steel, iron, and plastics, such that they emit 66% of the total GHG for this sector [17].

Plastics are polymers that are known for their strength and durability, thermal and insulation properties, resistance to stress, and chemical resistance [18,19]. Due to these properties, plastics are globally prevalent and are employed in various applications and sectors such as packaging, electronics, transportation, construction, and agriculture, to name a few [20]. Plastics from petrochemical origins accounted for around 4% of the total GHG emissions in 2015, such that 1.8 billion tonnes of CO_2e were released during the plastic lifecycle, not including end-of-life [21]. In 2020, it was approximated that 367 million tonnes of plastics were produced worldwide, a significant increase from the 1.5 million tonnes that were manufactured in 1950 [22]. It is anticipated that plastic production will grow by 100% by 2040 and by 150% by 2050 [23]. The increase in global production of plastics is respective to the increase in global population [17]. In terms of GHG emissions, annual emissions are estimated to reach 1.34 billion tons of CO_2e by 2030 [24].

As mentioned previously, the aim is to maintain the global average temperature ideally below an increase of 1.5°C [7]. The amount of GHG released from the plastic lifecycle is endangering this

goal: a total of 56 billion tons of emissions are expected to be reached by 2050, using 10-15% of the allotted emissions of the carbon budget [23,24]. It has therefore become increasingly important to come up with mitigating solutions for carbon emissions in industrial processes in general and plastic production in particular. These solutions include migration to bio-based plastics rather than fossil-based, relying on renewable sources of energy rather than fossil fuels, and developing technologies for carbon capture so that CO_2 is used as feed for plastics production [21,25].

The focus of this thesis is investigating a new pathway for low- and high-density polyethylene (LDPE and HDPE) production: the CCU-MTO pathway, which is based on the capture and conversion of CO_2 into methanol and then into olefins via methanol-to-olefins (MTO) process, and finally the conversion of olefins to polyolefins. The objective of this thesis:

- Modelling and simulating the process for LDPE and HDPE production in Aspen Plus following the CCU-MTO pathway
- Determining the greenhouse gas (GHG) emissions from polyethylene production via CCU-MTO pathway by conducting the life cycle assessment (LCA) of these processes in OpenLCA
- Comparing the emissions from the conventional method of LDPE and HDPE production to their production via CCU-MTO

2. Literature Review

2.1. Overview of polyethylene

2.1.1. Polyethylene molecular structure

A polyethylene molecule is a long chain of carbon atoms (backbone), linked together by covalent bonds, and two hydrogen atoms bonded to each carbon [26], as shown in Figure 2-1. Each polymer consists of a repeating unit; in this case it is -[CH_2-CH_2]$_n$-, such that n refers to the number of ethylene units linked together, or the degree of polymerization.
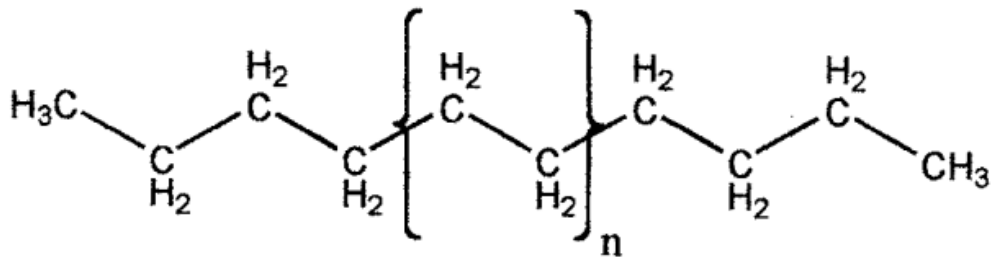
Figure 2-1: Polyethylene structural formula *[26]*

The degree of polymerization typically varies from 100 to 25000, and in turn, the molecular weight varies from 1400 to 3.5 million g/mol [26]. Consequently, the particle size distribution (PSD) varies as well. Not all polyethylene molecules have a linear structure and saturated bonds; some are branched and contain unsaturated bonds [26]. The degree and length of branching impact the density of the polymer, and consequently its crystallinity. Crystallinity refers to the alignment of polymer chains that influences hardness and density of a polymer [27]. The higher the concentration of branching, the higher the density and degree of crystallinity [26]. Other properties such as melting point, strength, toughness, and permeability are inversely affected by branching (and crystallinity); when branching increases these properties decrease [28,29].

2.1.2. Classification of polyethylene

Polyethylene is a thermoplastic which means that it can be melted and cooled repeatedly. It is also classified as being a semi-crystalline polymer. Crystallinity, which varies with branching, affects tensile strength, elasticity, and polarity of the polymer [30]. Depending on the degree of crystallinity, whether more amorphous or more crystalline, the polymer will exhibit different mechanical properties [26,30].

As mentioned in the previous section, branching affects density. Consequently, the most common way to classify polyethylene is based on density, such that the two major categories are low-density polyethylene (LDPE), and high-density polyethylene (HDPE) [31]. Linear low-density polyethylene (LLDPE) is also an important polymer, but it is not the focus of this thesis.

Low-density polyethylene consists of a backbone with long- and short-chain branches (LCB and SCB). LDPE usually has 2-3 LCB for every 1000 carbon atoms, and 10 SCB for every 1 LCB [30,32]. LCB promote a high melt strength where the polymer remains tough over a large temperature range [33]. SCB is responsible for the relatively low density and crystallinity (40-55%) which in turn decrease the melting point of LDPE [28]. The decreased melting point makes the polymer easier to process and more flexible, but still retains its toughness, making it suitable for diverse applications [26]. Free radical polymerization of ethylene under very high pressure produces LDPE [34]. Different industrial processes for LDPE production will be discussed in Chapter 2.

HDPE, on the other hand, is an almost completely linear polymer with minimal branching around five -CH$_3$- branches per 1000 carbon atoms, if any [34]. The more linear the polymer, the more brittle it is [30]. This leads to a high degree of crystallinity (70-80%) which is translated into a stiff (and therefore, brittle) and relatively impermeable polymer [26,28]. It is produced under low pressure conditions via coordination polymerization in the presence of a catalyst [34]. Table 2-1 summarizes the properties of LDPE and HDPE and their applications.

Table 2-1: Comparison of the properties and applications of LDPE and HDPE *[26,30,31,35,36]*

Poly-ethylene	Density (g/cm^3)	Structure	Properties	Applications
LDPE	0.91-0.94		- Easy to process - Flexible - Relatively tough	- Food packaging - Greenhouse covers - Juice/milk cartons - Squeeze bottles
HDPE	0.94-0.965		- Stiff - Brittle - Low permeability - Chemical and thermal resistance	- Grocery/trash bags - Liquid containment - Food storage - Piping systems

2.2. History of polyethylene production technologies

Some of the best discoveries happen to be accidents as is the case of polyethylene (PE). A German chemist, Hans von Pechmann, was credited with being the first to unintentionally synthesize polyethylene, in 1898, after a white powder was produced as a result of the decomposition of diazomethane [37]. The powder was later analyzed by two different scientists, and was found to be composed of carbon and hydrogen atoms with a sequence of -CH$_2$- repeating units [38]. These units were known as methylenes, and the product was consequently known as polymethylene. After that in 1929, Friedrich and Marvel came across a form of the same white solid discovered

by Pechmann but having a low molecular weight [37,39]. This powder was the yield of a reaction between ethylene with ethyl lithium and n-butyl lithium.

Their research paved the way for the production of commercial polyethylene. While studying the effects of high pressures on different chemical reactions in 1933, two chemists, Eric Fawcett and Reginald Gibson, came up with the first substantial method for the synthesis of PE at Imperial Chemical Industries (ICI) facility in England [40]. A mixture of ethylene and benzaldehyde, subjected to a temperature of 170 °C and a high-pressure range of 1700 to 2000 atm, led to the observation of a small quantity of white waxy substance at the inlet of the autoclave reactor, where the reaction was taking place [41]. The solid was identified as polyethylene. Unbeknown to both chemists, the oxygen they found in the reactor was the main initiator of the polymerization of ethylene; it was also the reason why they were unable to replicate their work [41]. In 1936, a researcher by the name of Michael Perrin, continued the work of his predecessors, and was able to produce relatively significant amounts of PE, after enhancing the reactor, and understanding the part the oxygen impurities had in initiating the polymerization [42]. The patent submitted by Fawcett, Gibson, Perrin, Paton, and Williams (1937) illustrated the free radical polymerization process initiated by low levels of oxygen (less than 10 ppm) present in the feed ethylene gas, that resulted in the formation of a branched PE having high molecular weight and low density (0.91-0.93 g/cc) [42,44,45]. This polymerization mechanism requires very high pressures in order to achieve polyethylene [44]. The generated PE proved to be tough and resilient, resistant to moisture, and an excellent insulator, resulting in the construction of the first PE plant in the UK in 1939 [40].

The importance of PE production was shaped by its use in World War II, where polyethylene was employed for the production of significantly lighter radar equipment [41]. The discovery of the importance of polyethylene by the United States government was imminent, and it was in 1943 that the ICI autoclave process developed by Fawcett et al. (1937) was licensed in the US, leading to the building of more PE production facilities because of the increase in demand [40]. The ICI autoclave system utilized oxygen as the initiator of the free radical polymerization of ethylene. Advances and evolutions in the field led to replacing oxygen with peroxides and transforming autoclave reactors into multi-zoned stirred autoclave reactors [46]. In 1943, a PE process that utilized tubular reactors instead of autoclave ones, was commercialized and developed independently by Union Carbide [45].

High pressure processes for the production of polyethylene dominated the industry from the time of its discovery in 1935 until the early 1950s, where new processes were implemented for the production of polyethylene by two different research groups, one in the United States by the Phillips Petroleum Company, and the other in Germany by the Max Planck Institute [44]. Standard Oil Company also developed catalysts for the production of polyethylene [47]. In 1951, the head researchers of the Phillips Petroleum lab, J. P. Hogan and R. L. Banks utilized chromium-based catalysts supported on silica to synthesize polyethylene at lower temperatures. While in 1953, Ziegler, the head researcher of the German group, uncovered a process for the production of polyethylene using a catalyst, a transition metal from Groups IV to VII, and a co-catalyst, an

organometallic compound from Groups I to III [45,48,49]. Commercial Z-N catalysts are typically heterogeneous, however, some are homogeneous, such as those developed from vanadium compounds [49]. Not all combinations of catalyst/co-catalyst are successful in polymerizing ethylene; the most common combination includes a titanium compound, such as titanium tetrachloride ($TiCl_4$) and an aluminum alkyl, such as triethylaluminium (TEA) [48,49].

The use of catalysts for the polymerization of ethylene by both groups produced two very similar linear polyethylenes, having a higher density than the polyethylene produced via low pressure processes [44,45,47]. This required the implementation of a new nomenclature to differentiate between the products of the two processes (high- and low-pressure). The main main distinguishing characteristic of the two products is density. Therefore, the polyethylene produced from high-pressure processes was known as low-density polyethylene (LDPE), while that manufactured via low-pressure processes came to be known as high-density polyethylene (HDPE) [45]. Other classes and subclasses of PE, also based on density, include linear low-density polyethylene (LLDPE), very low-density polyethylene (VLDPE), and ultra-high molecular weight polyethylene (UHMWPE), to name a few [32]. By changing the manufacturing process, catalysts and co-catalysts, and monomer types, polyethylene homopolymers or copolymers can be manufactured from ethylene gas, the main monomer [32]. The various methods to produce PE will result in different PE structures that can cater to diverse applications [32]. It should be noted that density is not the only quality that separates the diverse PE products. In fact, chain length, branching, and molecular weight also varied from one type to another, and they can all be attributed to having an effect on density, and other physical, chemical, and mechanical properties.

2.3. Industrial polyethylene processes

2.3.1. LDPE production (High pressure processes)

In the high-pressure LDPE production process, both long-chain and short-chain polymers are produced [32]. As mentioned previously, the polymerization process to achieve LDPE is a free radical polymerization technique. Process conditions involve very high temperatures (80-300°C) and pressures (100 to 350 MPa), that vary based on the type of reactor used, i.e., autoclave or tubular [32,41,47,50]. The reaction begins in the presence of an initiator, typically oxygen or a peroxide [32,47]. A free radical of ethylene comes into contact with ethylene, and the chain continues to grow, forming polyethylene [32].

2.3.1.1. Autoclave process

Continuous-stirred tank reactors with agitators, with an aspect ratio (height/diameter) of 15 to 25 are typically used in the autoclave process [47,49] [32,41]. Moreover, the walls of the reactor are of significant thickness, in order to withstand the severe process conditions (150-315 °C and 100 to 200 MPa) [32,49,51] Due to the exothermic nature of the polymerization reaction and the restricted ability of autoclaves to remove heat, certain measures must be taken in order to prevent the formation of a thermally unstable reaction system, such as the decomposition of ethylene into

methane, hydrogen, and carbon, known as a runaway reaction [41,52]. This can be done by introducing the feed at very low temperatures to uphold the target reactor temperature, consequently eliminating the heat of the polymerization reaction [32,41,47]. In addition, all autoclave reactors are equipped with relief valves that release the products of ethylene decomposition into the atmosphere and avoid the eruption of the reactor vessel [41,52]. Average residence time ranges from 20 to 80 seconds [50]. e

The standard autoclave process consists of a compression stage of ethylene, a reaction or polymerization stage, and a separation and recycling stage [41]. The compression stage consists of multiple compressors, where, any unreacted monomer from the low-pressure separator is recycled and mixed with the ethylene feed, before being sent to a primary compressor [41,53]. The discharge of the primary compressor is fed into the hyper compressor, along with the high-pressure separator stream [41,53]. The mixture is then pressurized to a pressure ranging from 120 to 240 MPa, which is the reactor pressure [32,54]. The outlet of the secondary compressor, i.e., the compressed ethylene, is introduced into the autoclave reactor along with the chosen initiator for the polymerization reaction to take place [32,41,53]. Consequently, the products are sent to the separation units in order to increase the mass purity of LDPE and recycle the unreacted monomer, ethylene, back into the system [32]. The conversion of monomer to polymer varies from 10 to 30% [32,41,47]. A process that requires very high pressures, and is consequently, very expensive, only to have such a low conversion rate, is not deemed a proficient process for PE production [41].

2.3.1.2. Tubular process

A plug flow reactor (PFR) is used for the production of LDPE in this case. The reactor is typically between 500 and 2000 m in length and 3 to 9 cm in diameter, and has numerous points of entry for introducing the initiator [30,49]. Reactor operating conditions include pressures from 200 to 350 MPa and temperatures between 170 and 330 °C [49,51,54]. Once again, cooling is required in order to remove heat of the reaction. In this case, it is done by cooling jackets, as well as introducing cool ethylene feed into the reactor [30].

In terms of production stages (compression, polymerization, separation and recycling), they are similar to those of the autoclave process, as shown in Figure 2-3 [32]. Relative to the length of the reactor, the conversion per pass is low with a maximum of ~30-35% [30,32,41,55]. In order to increase the yield, the recycling of unreacted ethylene must be added [55].
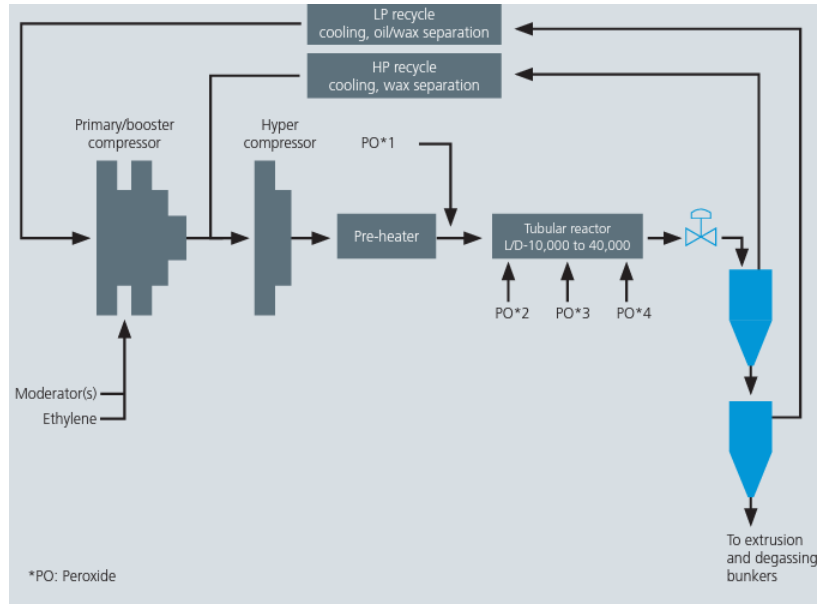
Figure 2-2: Schematic of ethylene polymerization to LDPE in a tubular reactor [56]

Similar to the autoclave process, the low-pressure stream, from the LPS, is mixed with the feed and compressed [55]. Then, the output of this primary compressor, and the unreacted monomer from the HPS, are pressurized via the hyper compressor to a discharge pressure of 200-300 MPa, depending on the reactor operating conditions [55].

While both autoclave and tubular reactor systems require elevated temperatures and pressures to produce LDPE, the production cost of the autoclave systems is typically higher than that of the tubular reactors owing to their higher capital costs and lower conversion rate [41]. Consequently, in this thesis, the process is simulated based on the tubular process. A more detailed process description will be given in Chapter 4.

2.3.2. HDPE production (low-pressure processes)

The pressures involved in the production of HDPE are relatively lower than those involved in the formation of LDPE. The reaction mechanism follows a coordination polymerization. It involves several components: the monomer ethylene, the catalyst, the solvent, and the chain transfer agent. The polymer properties can be modified by varying the solvent type and concentration, or the addition of a co-monomer [46].

There are three processes that may result in this form of the polymer, and they include gas-phase, solution, and slurry processes. Operating conditions are milder than processes for LDPE production, but they differ between these three processes [57].

2.3.2.1. Gas-phase polymerization

In the gas-phase process, the reaction takes place in a fluidized bed reactor, with an aspect ratio of around 7 and a height that reaches 25m, such that ethylene (gas) is converted into a solid polymer [31,32,50]. In addition to ethylene, the raw materials involved include hydrogen gas, which controls the molecular weight, a catalyst, and a co-catalyst [50]. The catalyst and co-catalyst are fed directly into the reactor [54]. The pressure is typically between 1.5 and 2.5 MPa, and the temperature should be kept below 115 °C in order to avoid melting the solid polymer [32,50]. To avoid pressure build-up in the reactor, a discharge valve is added to allow for intermittent discharge of polymer [54]. After exiting the reactor, the polymer enters a separator so that the gases are recycled back into the system, and the high-purity polymer is subjected to additives before being formed into pellets [32]. Typical catalysts for this process are the Z-N catalysts and chrome-based catalysts [54]. To control and maintain the reactor temperature, a cooled gas in the form of a hydrocarbon, such as 1-butene or 1-hexene, is injected into the reactor [54]. This co-monomer has an inversely proportional effect on the polymer density; adding more co-monomer, decreases the polymer density. Figure 2-4 is a simple diagram of gas-phase polymerization of ethylene.
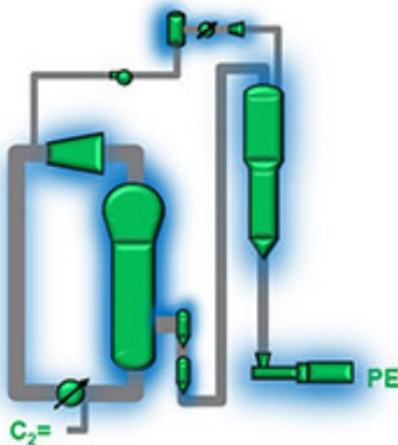
Figure 2-3: Gas-phase polymerization schematic by Univation Technologies [58]

2.3.2.2. Solution polymerization

As for the solution process, polymerization takes place in one or two autoclave reactors in series [31]. This is a high-temperature process, such that the operating temperature may reach 250°C, in order to keep the polymer dissolved in the solution [32,50]. The operating pressure is higher than gas-phase processes; it can reach 10 MPa [31,50]. The raw materials, ethylene and hydrogen, are dissolved in a hydrocarbon solvent, forming a diluted solution [31,32]. The polymer is then separated from the solvent and any unreacted monomer, before being pelletized [32,50]. The reactors are operated adiabatically, so there is no need to account for heat removal [50]. However, in order to avoid overheating of the reactors, the monomer and solvent are cooled before being recycled back into the system [31,32]. Z-N catalysts are used in solution processes [31,32,50]. Solution polymerization processes can also produce LLDPE, by adding a co-monomer, typically

an α-olefin, usually 1-octene [31,32]. Figure 2-5 shows a simplified diagram of the solution polymerization process taking place in two autoclaves [32].
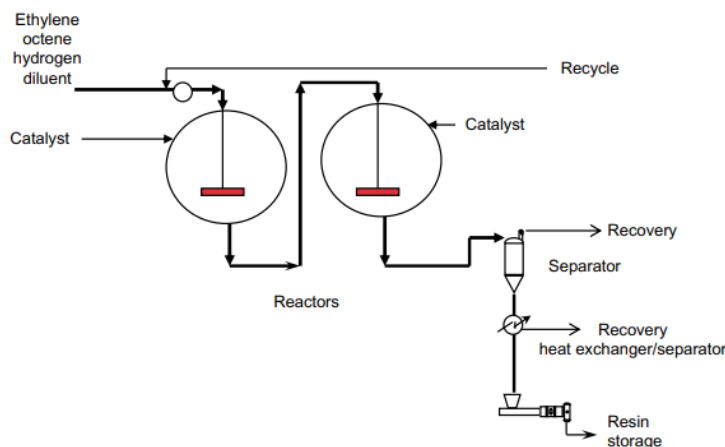
Figure 2-4: Diagram of solution polymerization [32]

Even though solution polymerization has short residence times and does not require complex heat removal mechanisms, it requires high capital and operating costs for product separation that overshadow these advantages [31,50].

2.3.2.3. Slurry (suspension) polymerization

Slurry polymerization processes are the oldest and most commonly used and developed processes to synthesize HDPE [31,32]. In this case, the reactors used are either continuous stirred-tank reactors (CSTRs) or loop reactors [32]. If CSTRs are used, there are at least 2 reactors used, either in series or parallel, depending on the desired polymer specifications, and if loop reactors are used, they are usually made of multiple loops and reactors (the number of loops also influences polymer properties) [54]. The process involves the monomer ethylene, hydrogen, and a heterogeneous catalyst dissolved in a hydrocarbon diluent [31,32]. The difference between the two is the type of diluent used. If hexane is used as diluent, it does not allow for the production of LLDPE, only HDPE [31]. This is because the amorphous portion of LLDPE dissolves in hexane and causes reactor fouling [31]. On the other hand, in loop processes, such as those licensed by Chevron-Phillips, isobutane is used as solvent and amorphous substances are less soluble in isobutane than hexane, allowing for LLDPE production [31,59]. For both processes, loop or CSTR, the produced polymer should be in solid form, such that it is suspended in the liquid for easy separation [32]. Therefore, operating temperature of both processes should be less than the melting point of the polymer; typically less than 100°C [31,32]. Pressure is significantly less than what is used for LDPE production but varies between processes. Residence times are typically between 45 minutes and 2 hours [31].

The polymerization of ethylene into HDPE is an exothermic reaction, and consequently, cooling jackets surround the reactor, loop or CSTR, to allow for heat removal [31,32]. Once the polymer

is formed, the slurry is removed. The polymer is separated from the solvent and any unreacted monomer before being pelletized [32]. Ethylene and diluent are recycled back into the system. A co-monomer may be added to control polymer density. Typical catalysts are Z-N catalysts, although chromium-based catalysts can also be used [32]. A simplified schematic of the loop process is found in Table 2-6.
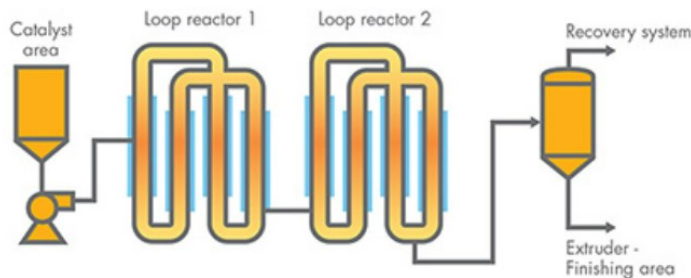
Figure 2-5: Schematic of two loop reactors in series [60]

The presence of a solvent in slurry polymerization requires extra purification and separation units, making it more expensive than gas-phase polymerization [61]. Regardless, this approach remains dominant in the market, as it offers a number of desirable features, such as moderate process conditions, high conversion, and easy operation and heat control [62]. In addition, as mentioned by Daftaribesheli [61], the majority of catalysts that are developed for HDPE production are suitable for the slurry polymerization approach. Consequently, in this thesis, slurry polymerization in 2 CSTRs in series was chosen for HDPE production, and a more detailed process description and figure will be shown in Chapter 4.

2.4. Global polyethylene production and emissions

Million tonnes of plastics are produced annually worldwide. Out of the 380 million metric tons of plastics produced in 2015, 115 million metric tons were polyethylene (PE), which is a little over 30% of the global plastic production, making it the most manufactured polymer [63]. The various applications of polyethylene and its ease of fabrication, make it one of the most popular plastics. It can be used in packagingother , plumbing, and automotive sectors [64]. Moreover, polyethylene can be used in the construction sector as an alternative to the traditional materials. The distinct properties of this polymer allow for these diverse applications. Different technologies and conditions have been employed by different researchers in the production of polyethylene, and this has led to the development of various polyethylene grades, typically classified based on density. Two of the most common grades include low-density polyethylene (LDPE), high-density polyethylene (HDPE). Other grades of PE also exist, however, compared to the vast quantities of HDPE and LDPE being produced, the other types warrant little interest (except for linear low-density polyethylene (LLDPE)).

Various literature have been concerned with conducting life cycle assessment on LDPE and HDPE produced from fossil fuels [17,66–68]. The results vary based on the boundaries chosen, electricity source, and software and databases used. However, what is common between all the literature results is that LDPE emissions are higher than HDPE emissions, because the former requires higher temperatures and pressures.

According to a report published by Franklin Associates to the American Chemistry Council (ACC) [69], only 13% of the energy required for the production of LDPE from fossil fuels is related to the polymerization of ethylene, the remainder comes from the extraction of raw materials, electricity generation, and the production of the olefin ethylene. Another report determined that 7% of the total energy needed to produce fossil-based HDPE comes from the polymerization itself [70]. Additional both reports demonstrated that the majority of emissions is from the production of ethylene and not from the polymerization, which will be discussed in Chapter 3.

3. Ethylene production pathways

The predominant framework in the plastic chain is the linear economy, also referred as "take-make-use-dispose economy," in which the resources, energy, and products, are used once before being discarded [71]. Apart from producing greenhouse gases, this system consumes a significant amount of fossil fuels and generates a lot of other pollutants, making it unsustainable [71]. Therefore, to reduce the impact of CO_2 emissions on the environment and human health, different strategies have been proposed to minimize the carbon footprint of the plastic chain. As mentioned in Chapter 2, emissions are mainly released during olefins production.

Olefins can be produced from various feedstock such as oil, natural gas, coal, biomass, and CO2, Various technologies have been developed for olefin production. The focus of this thesis is on the production of ethylene, which is the main feedstock of HDPE and LDPE polymers. Zhao et. al (2021) and Reznichenko and Harlin (2022) analyzed different pathways for olefin production [72,73]. The main processes include steam cracking (SC), ethanol dehydration, methanol-to-olefins (MTO), Fischer-Tropsch-to-olefins (FTO), and oxidative coupling of methane (OCM) [72,73]. Figure 3-1 is a simplified flowchart of the different pathways to produce ethylene and includes the main feedstock, its processing technique, the intermediate product which will be converted to ethylene, and the production process of the olefin.
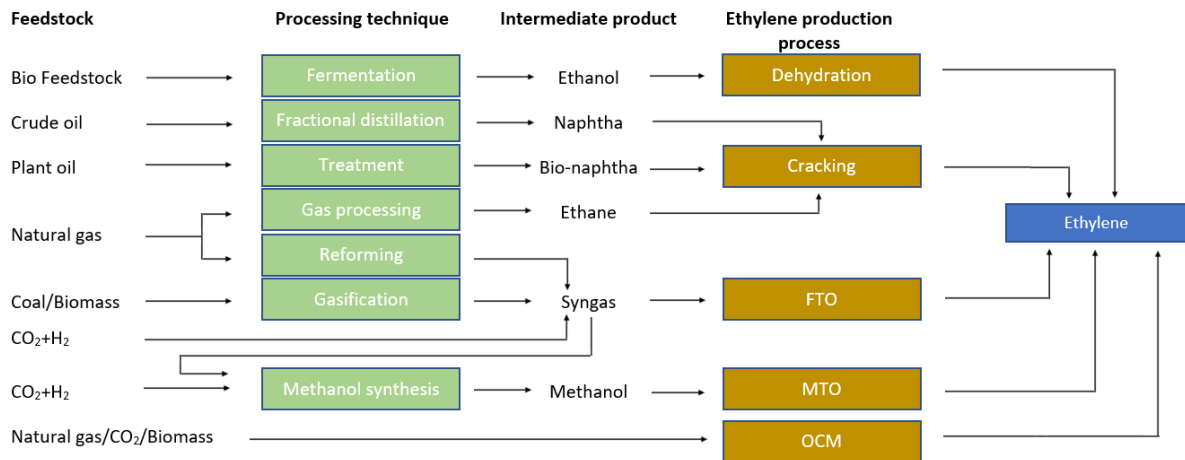
Figure 3-1: Pathways of polyethylene production

3.1. Traditional Pathways

3.1.1. Steam cracking

Steam cracking (SC) is one of the most established technologies for the production of ethylene and propylene [74–76]. The most common hydrocarbon feedstocks include naphtha and ethane, even though bio-naphtha is also used. They are subjected to heat in order to break down the carbon bonds, and consequently, produce light olefins and other by-products, such as butane and gasoline

[74,75,77]. A typical SC plant involves three main sections: cracking and quenching, compression, and product recovery [72,78]. The first section involves the introduction of steam and feedstock to a tubular reactor (cracking furnace) to undergo cracking at high temperatures (500-680°C) in the absence of oxygen [75,76,79]. To trigger the endothermic conversion of feedstock into unsaturated olefins, mainly ethylene and propylene, the reactor is suspended in a gas furnace, such that the mixture reaches temperatures ranging from 750 to 875°C [74–76,78,80,81]. Quenching of the effluent gas of the furnace is then done via transfer line exchangers (TLEs), such that the heat is transferred to the water/steam portion of the exchanger, decreasing its temperature to as low as 400°C [78,82]. The recovery section involves the separation of the desired products, ethylene and propylene (only if naphtha or bio-naphtha are the feedstock), from the other hydrocarbons [78]. A simplified flowsheet of naphtha steam cracking is observed in Figure 3-2.
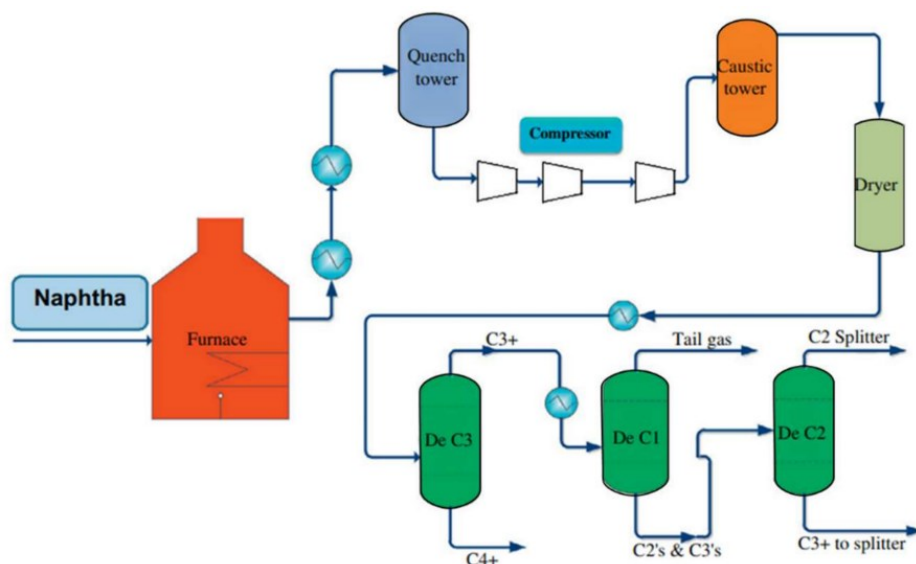
Figure 3-2: Simplified flowsheet of naphtha steam cracking [83]

The development of shale gas in the United States has led to the abundance and availability of ethane at low cost, shifting the focus from naphtha cracking to ethane cracking [75]. Even though the cracking of both feedstocks, ethane and naphtha, follow almost identical procedures, ethane cracking does not require a separation process as demanding as naphtha cracking, since only ethylene is produced, meaning that ethane cracking requires less capital than naphtha cracking [75].

In steam cracking, the main product is ethylene while propylene is considered an unintentional by-product. Therefore, when referring to emissions or energy demand of steam cracking, the results are in terms of ethylene [72,78]. According to Ren at al. (2006), both naphtha and ethane cracking are highly energy-intensive, such that the heat required by each, respectively, ranges from 20-40 and 17-25 GJ/t of ethylene [78,81]. Additionally, the CO_2 emissions, in tonne of CO_2/tonne of ethylene, resulting from naphtha cracking are between 1.8 and 2, and between 1 and 1.2 for ethane cracking, resulting in 300 million metric tons of CO_2 per year [74,78,81,84].

The reason these technologies are so prevalent is due to their low cost compared to other processes [17]. In addition, these processes are also better established compared to the newly developed processes [17]. However, in the long term, neither steam cracking nor catalytic cracking are environmentally viable routes for olefin production because of there high CO_2 emissions [17].

3.1.2. Ethanol to ethylene

Up util the 1940s, ethylene was produced via the dehydration of ethanol [85]. The majority of ethanol is produced from different agricultural sources such as crops that are starch- or sugar-rich, algae, and lignocellulose [73,86,87]. In addition to being a solution that limits dependency on fossil fuels, the incentive behind using biomass as feedstock is to decrease GHG emissions [71].The dehydration of ethanol into ethylene is an endothermic reaction that takes place at temperatures between 300 and 500°C in the presence of a catalyst [86]. However, before reaching dehydration, three steps must be followed: obtaining the raw materials, fermentation of raw materials into ethanol, and lastly purification and dehydration of ethanol [87]. Regardless of the biomass source used, these three steps are followed to produce bio-ethylene, the only difference is the process that is used to generate ethanol, as it depends on the source [87]. Various catalysts have been explored to decrease process conditions and increase the yield; while successful, they are not yet developed for the industry level [88].

The cost of the process, while not dependent on fossil fuel prices, varies based on the availability of biomass [87]. That being said fossil fuels are much more abundant, and consequently steam cracking plants dominate the industry in comparison to ethanol to ethylene plants [88]. Although more plants are either under construction or planned, they cannot compete with steam cracking plants; the largest ethanol to ethylene plant located in Brazil produced 0.2 million tons of ethylene per year, compared to 2.9 million tons annually from a steam cracking plant in Taiwan [88,89]. The main advantage of bio-ethylene, other than shifting focus to greener methods of production, is that it is chemically identical to ethylene, meaning it can be used by the same equipment [89].

3.2. Novel Pathways

3.2.1. Fischer-Tropsch to Olefins (FTO)

FTO is an exothermic catalytic process that uses syngas, derived from coal, biomass, natural gas, or CO_2, and converts them into a wide variety of products, mainly paraffins, olefins, and a trace of oxygenates [73,75,86]. Equations 3-1 and 3-2 are the main reactions that take place for the production of olefins and paraffins respectively [90].

$$nCO + 2nH_2 \rightarrow C_nH_{2n} + nH_2O \quad \text{Equation 3-1}$$

$$nCO + (2n + 1)H_2 \rightarrow C_nH_{2n+2} + nH_2O \quad \text{Equation 3-2}$$
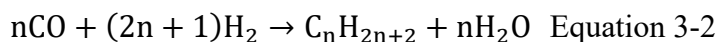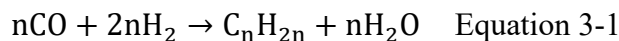
The components of the mixture produced from this process are dependent on the operating conditions, the type of catalyst used, the type of reactor, and the ratio of H_2 to CO [72]. To combat

the low selectivity of FTO towards lower olefins, high operating temperatures as well as metal catalysts are used [72,73,91,92]. The high temperature and use of an iron catalyst, shift the selectivity towards the desirable products [93–95]. This process is known as High Temperature Fischer-Tropsch (HTFT). This process typically takes places in a fluidized bed reactor with an operating temperature between 320 and 350°C [96]. A simplified diagram of the process, adopted and edited from [91], can be seen in Figure 3-3.
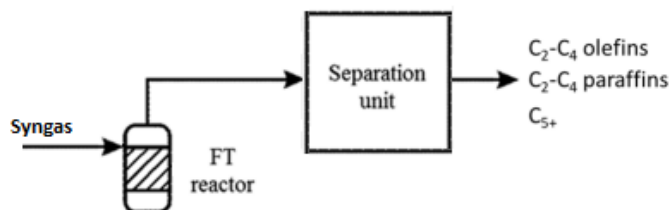
Figure 3-3: FTO simplified flowsheet [91]

Syngas is introduced into the reactor where it is transformed into different hydrocarbons with the help of a catalyst. In order to separate the produced hydrocarbon mixture, a separation unit is required. The first step involves the removal of water, and with it the oxygenates [91]. C_{5+} compounds are the removed via a distillation column, followed by a CO_2 removal process. The paraffins and olefins are then introduced into multiple separation columns, such that first methane is separated, followed by C_2 compounds, and then C_3 and C_4 compounds [91]. Not all syngas is reacted, and even though recycling the syngas would increase the conversion rate, investment costs would also increase because of the demand for a larger FTO reactor and separation units [95]. Despite various efforts for improving the selectivity of FTO to lower olefins, this process requires high capital cost that come with equally high risk [75].

3.2.2. Oxidative coupling of methane

Oxidative coupling of methane (OCM) is a process through which methane mixed with oxygen and subjected to high temperatures, in the presence of a catalyst, is converted to ethane (Equation 3-3), and then ethylene by thermal dehydrogenation (Equation 3-4) [73,97]. Hutchings et. al (1989) mentioned the formation of higher hydrocarbons, such as propane and propylene, but at much lower quantities that C2 hydrocarbons, as well as traces of methanol and ethanol, contributing to undesirable side reactions [98,99]. This process does not rely on syngas as an intermediate product, but rather directly converts methane into ethylene, and is therefore less energy-intensive and less expensive than FTO [73,75,97,100].

$$2CH_4 + 0.5O_2 \rightarrow C_2H_6 + H_2O \quad \text{Equation 3-3}$$

$$C_2H_6 + 0.5O_2 \rightarrow C_2H_4 + H_2O \quad \text{Equation 3-4}$$
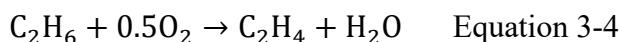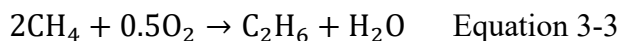
Methane can be obtained from various sources: natural gas which is formed of 70-90% methane and can be used as feed directly, and biomass, and CO_2 (and H_2) which are more complex processes [73].

17

Despite years of research, only 10-25% of methane has been converted to ethylene via OCM [101]. This low yield has made OCM economically unfeasible, and is the reason why it is still not commercially available [73,101]. This process has very low CO_2 energy emissions (0.25 tonne CO_2/tonne of HVC), however, its low selectivity to ethylene leads to high chemical CO_2, from the side reactions [74]. Therefore, in order for this process to compete with steam cracking, significant improvements must be made to the catalyst to increase selectivity to ethylene, as well as make modifications to the reactor design, to accomodate this highly exothermic reaction [74,75].

3.2.3. Methanol to Olefins

MTO is a novel process that involves the transformation of methanol into primarily ethylene and propylene. Methanol can be obtained from multiple feedstock can be used for this process: coal, natural gas, biomass, and CO_2 [73,75]. The conversion of methanol into olefins is an exothermic reaction that takes place in a catalytic reactor in the presence of a catalyst. Typical operating conditions involve a temperature between 350 and 500°C and a pressure range 100-300 kPa [102,103]. The product of the reactor is sent to a separation section where CO_2 is removed and each of ethylene and propylene is separated from the other hydrocarbon products [103]. A more detailed description will be addressed in Chapter 4. Figure 3-4 shows a simple diagram of the MTO process.
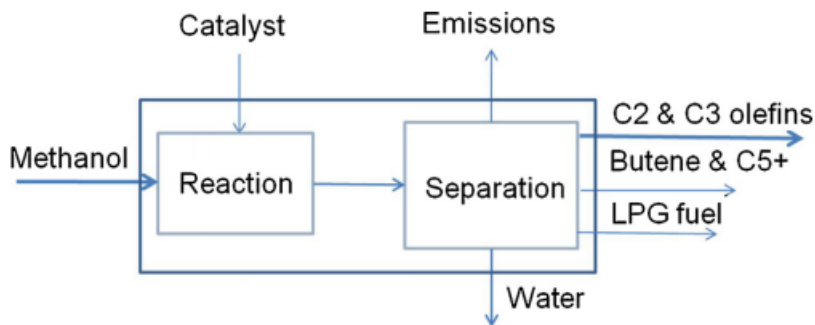
Figure 3-4: Diagram of MTO process [103]

3.3. Carbon capture and plastic production

Circular economy is a "restorative and regenerative" framework [23,71]. It includes strategies that will allow for the maximum use and regeneration of resources, materials, and products, whether in the same process or a different one, in an effort to decrease and ultimately eliminate the negative impact that plastics have on the environment [71,104].

Carbon capture is an alternative approach that addresses the issue of the plastic chain's carbon footprint and fully integrates plastic production in the circular economy framework [17]. The captured CO_2 can be sequestered in the storage fields or alternatively utilized as the feedstock to produce value-added products (CCS and CCU, respectively). There are some challenges to CCS, including a lack of financial incentive, due to the high costs associated with capture, transportation,

and storage of CO_2, and also a lack of appropriate underground storage sites in many areas capable of securely storing large quantities of CO_2 [105].

Instead, CCU is an alternative option where conversion methods can be applied in order to achieve various products, such as fuels, minerals, and polymers to name a few [106]. CCU has tremendous potential as a component of a sustainable circular economy solution for minimizing the consequences of climate change caused by hydrocarbon burning, particularly when combined with other renewable energy sources. According to the research conducted by Khamlichi and Thybaud, the conversion of CO_2 to produce methanol is one of the three most favorable pathways among more than 30 CO_2 conversion pathways [106]. Additionally, since methanol is a primary component for different fuels and chemicals, developing the CCU-methanol process is critical [105]. Khojasteh et al. compared the lifecycle GHG emissions of different methanol production processes and concluded that CO_2 hydrogenation is the most viable one in areas that have access to low carbon or renewable electricity [105].

3.4. CO_2 emissions from various pathways of ethylene production

A study by Zhao et. al evaluated the amount of CO_2 emissions, in tonnes, from different ethylene production pathways (different feedstock and different processes), per tonne of ethylene [86]. The results are displayed in Table 3-1.

Table 3-1: Life cycle CO_2 emissions from different ethylene production pathways (tCO_2/t ethylene) [86]

Pathway	Emissions
NG-SC	1.3
Coal-MTO	8.5
NG-MTO	3.4
CO_2-MTO	-0.02
Biomass-MTO	-1.3
Coal-FTO	20.5
Biomass-to-ethylene	-0.6

From Table 3-1 it can be seen that coal-FTO emits the most CO_2 out of the studied pathways, while the least emissions are released from the biomass-MTO pathway, which showcases negative emissions. Additionally, negative emissions were recorded by CO_2-MTO and biomass-to-ethylene pathway (ethanol dehydration pathway). The other MTO pathways, release less amounts of emissions than the coal-FTO pathway, but more than the steam cracking of natural gas pathway. Even though the least emissions were recorded by the pathways which rely on biomass as feedstock, they are not the most desirable as mentioned previously. Eliminating NG-SG, coal-FTO, and bio-based pathways, the only pathways left are those based on MTO. Further elimination

gets rid of coal-MTO and NG-MTO as they emit 8.5 and 3.4 tCO_2/t ethylene. The most desirable option is, therefore, CO_2-MTO, with negative CO_2 emissions per tonne of ethylene. This is validated by the study by Khojasteh- Salkuyeh et. al [105].

4. Process description and design

4.1. Process description

A simplified block flow diagram of the pathway is illustrated in Figure 4-1. High-purity CO_2 is compressed and sent to the methanol synthesis unit, where it is combined with hydrogen (from the electrolysis unit) to make methanol. The Lurgi two-stage reactor system is used for methanol production [105]. The methanol product is then sent to the methanol-to-olefins unit to produce the ethylene and propylene olefins [107,108]. Finally, the ethylene product is sent to the polymerization unit, where two different pathways are considered for low-density and high-density polyolefin production.
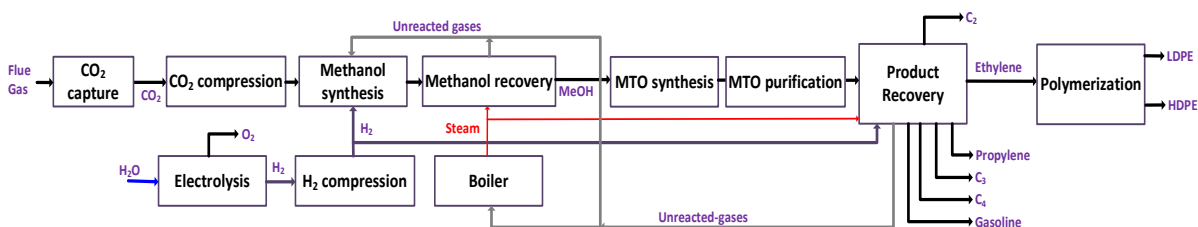
Figure 4-1: Block flow diagram of the CCU-polymers process

The proposed methodology involves process design and simulation, followed by lifecycle assessment to determine the environmental impacts of each product. The process simulation of both LDPE and HDPE pathways is conducted using Aspen Plus V12.1. The simulation results are then used to establish the life cycle GHG emissions of each polymer based on various methanol production pathways across different Canadian provinces and compare them to their respective conventional pathways.

4.1.1. Methanol production

The primary process for methanol production is based on the CO_2 capture and hydrogenation in the Lurgi two-stage tubular reaction system (Figure 4-2). This process is based on that developed by Khojasteh-Salkuyeh et. al [105]. To obtain the high purity CO_2 (99.5%) required for methanol production, flue gas from a cement kiln is passed through a direct contact cooler (DCC) to remove water vapor and any undesirable particles before being sent to a two-stage membrane separator. The required hydrogen is produced by using a PEM electrolysis unit, followed by the compression and water removal train to obtain high purity (99%) hydrogen [105]. The hydrogen and CO_2 mixture is then sent to the dual-stage quasi-isothermal steam-raising fixed bed Lurgi MegaMethanol reactor, which can provide better temperature control and heat recovery compared to other methanol synthesis technologies [109]. The recovery section involves two separator columns, first to remove any unreacted gases, and then to eliminate moisture and impurities to achieve methanol having a mass purity of 99.85%. The simulation and design parameters of this process are presented in our prior work [105], which is omitted here for brevity.
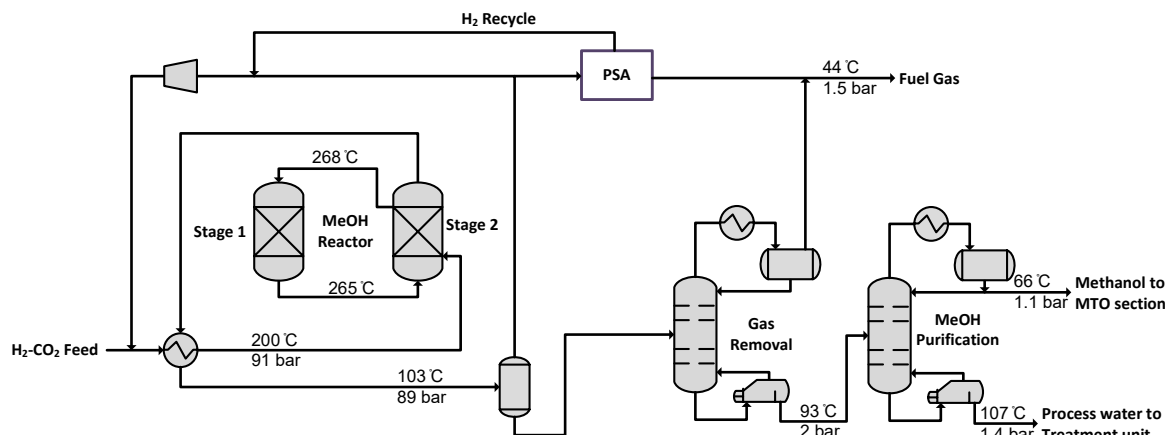
Figure 4-2: Process flow diagram of the methanol production unit (see [105] for more details).

4.1.2. Olefins production

Figure 4-3 depicts a simplified process flowchart for the conversion of methanol to olefins. This process is simulated using the UOP/Norsk MTO technology, which consists of a fluidized-bed catalytic reactor (using SAPO-34 catalyst), connected to a fluidized-bed regenerator to recycle the catalyst [110]. The feed methanol is preheated and then transferred to the MTO reactor, which works at 530 °C and 3.5 bar [111]. The conversion and selectivity of the reactor are adopted from the experimental data provided for the SAPO-34 catalyst and the Intratec Report [112,113]. The solid catalyst is cycled to the regeneration reactor, where the coke formed on the surface of catalyst is combusted with air. After gas product cooling, further water condensation and methanol removal are conducted using the quench tower and methanol recovery column [114]. The quench tower removes unreacted methanol from the gas product stream and also reduces the water content of the product gas stream to less than 5%. The collected liquid stream is sent to the methanol recovery column, which recovers 90% of the unreacted methanol with at least 80% purity. The gas stream from the quench tower is compressed and sent to the hydrocarbon stripping column to recover 99% of the light hydrocarbons [114]. The olefin stream is sent to a CO_2 absorber to remove CO_2 using caustic washing, before being sent to multiple columns to separate each of ethylene, ethane, propylene, and propane from the remaining heavier olefins and hydrocarbons [115]. It should be noted that the heat recovery of the entire plant is conducted using the INTEGRATION software, developed by CanmetENERGY [116]. However, for the purpose of clarity, the updated heat exchanger network is not illustrated.
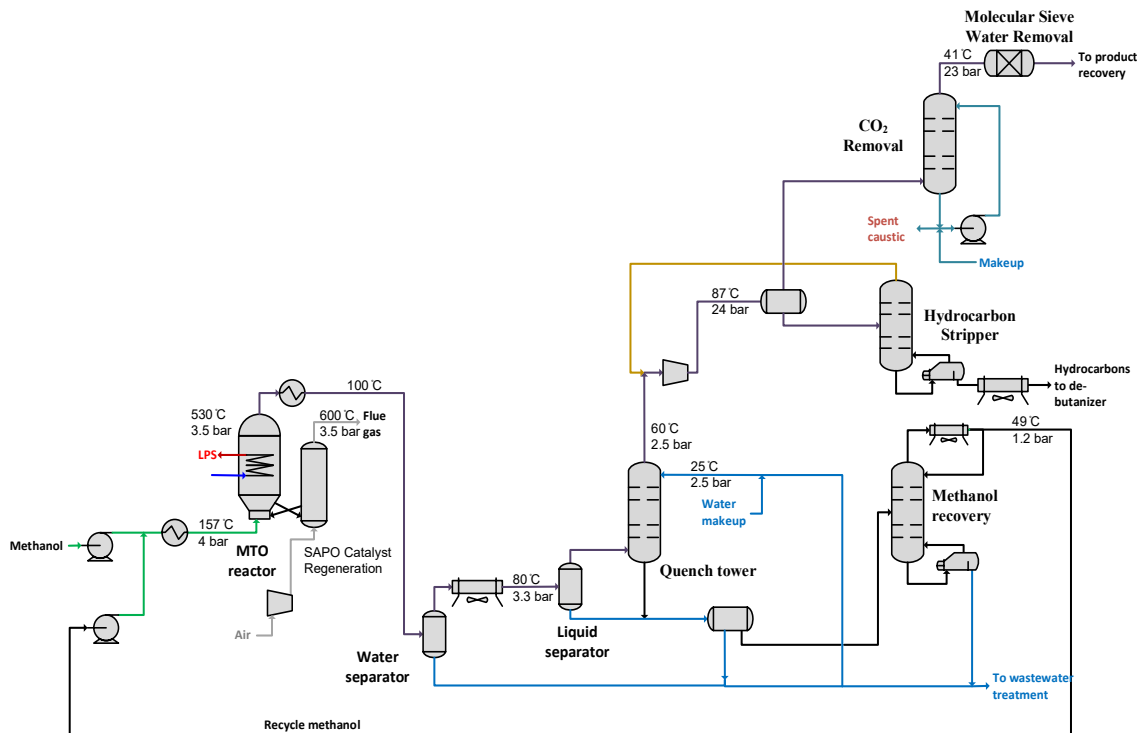
Figure 4-3: Process flow diagram of the MTO reactor and product gas cleanup sections

The process flowchart of the product recovery section is depicted in Figure 4-4, which is modelled using the process data provided by Intratec Report [113]. Ethane and lighter hydrocarbons are separated from heavier hydrocarbons in the DeEthanizer column. The DeEthanizer column is designed to send 99.9% of the ethane to the top product stream and 99.9% of propylene to the bottom stream. A hydrogenation reactor is then used to convert the trace amount of acetylene in the top stream to ethane. The gas product is then sent to the deMethanizer column to remove methane from the ethylene and ethane mixture. The deMethanizer column removes 99.5% of methane and also recovers 99% of ethylene from the top gas stream. The ethylene-ethane mixture is sent to the De-Ethanizer column, where 98% of ethylene is recovered with a mass purity of 99.5%. The bottom liquid stream of the DeEthanizer column is sent to Depropanizer, where propylene and propane are separated from the heavy hydrocarbon mixture. The top stream is sent to the C3 Splitter column to purify propylene. This column is designed to achieve a propylene recovery of 85% with mass purity of 99.5%. The bottom stream is sent to the DeButanizer column to separate butane from C_5^+ mixture. The C_5^+ stream can be sold as the pyrolysis gasoline product, after further purifications. The UUNIQAC-RK property method is used for the simulation of all MTO units, except for the CO_2 removal section, where the ELECNRTL model is used. These property methods are validated using the National Institute of Standards and Technology (NIST) database.
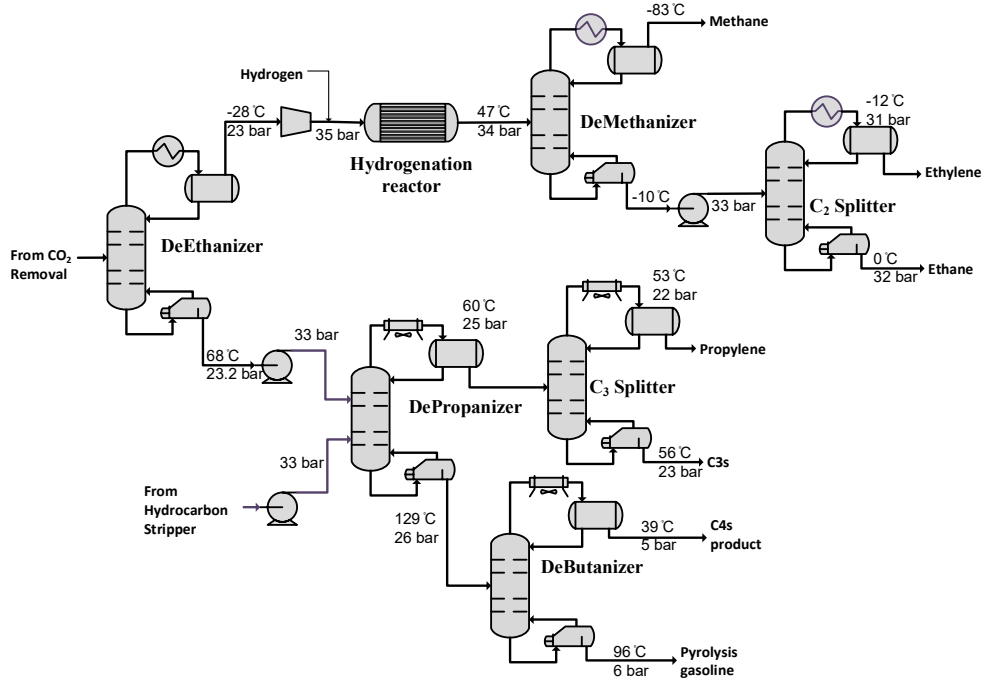
Figure 4-4: Process flow diagram of the MTO product purification section

4.1.3. LDPE production

4.1.3.1. Process description

While both autoclave and tubular reactor systems require elevated temperatures and pressures to produce LDPE, the production cost of the autoclave systems is typically higher than that of the tubular reactors owing to their higher capital costs and lower conversion rate [41]. Consequently, the process is simulated based on the Lupotech-T licensed technology by LyondellBasell for the LDPE production, using ethylene feedstock and tubular reactor [117]. The reaction takes place in a jacketed tubular reactor with multiple initiator injection points and coolant streams [118]. Benzoyl peroxide and di-t-butyl peroxide are used as initiators, and they must be stored at low temperature to prevent decomposition [49]. The reactor is divided into four reaction zones (plug flow reactors (PFR)). Details of the design parameters and process simulation assumptions are listed in Table 4-1. The Sanchez-Lacombe equation of state (POLYSL) is used for the simulation of all PFRs. The process is divided into three stages, compression, reaction, and separation and recycling, and is shown in Figure 4-5 [41].
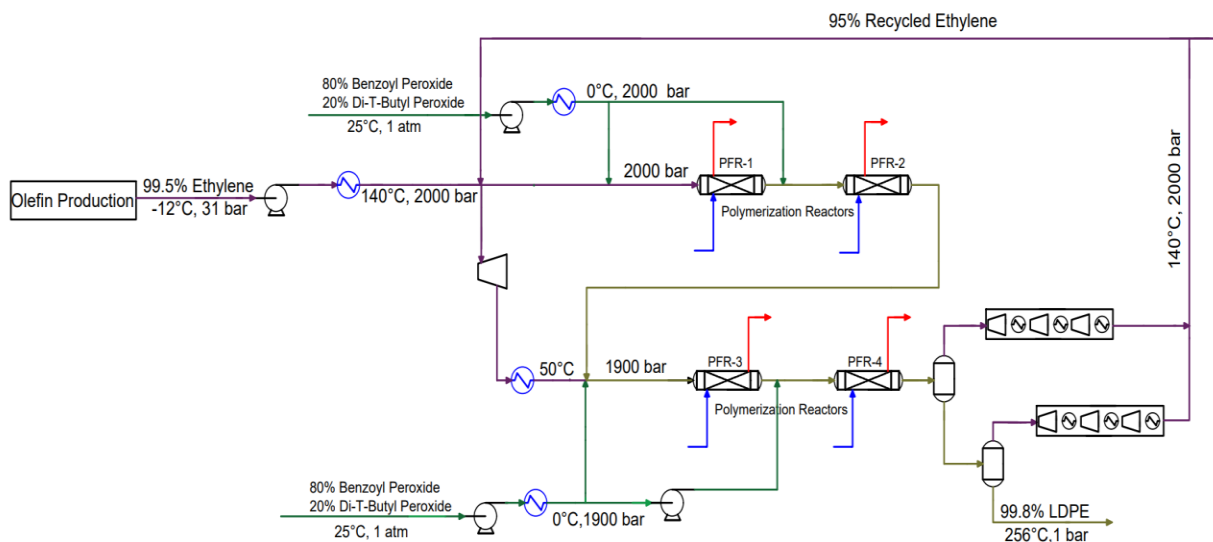
Figure 4-5: Simplified process flow diagram of the modified LDPE production process

Because LDPE production is a high-pressure process, the ethylene stream from the olefin production unit is compressed and heated to reach 140°C and 2000 bar. Around 60% of the feed is sent to the first zone, while the rest are sent to the second. The stream heading to the second zone is further modified to reach a temperature and pressure of 50°C (to ensure the input stream temperature to PFR-3 does not exceed 150°C) and 1900 bar, respectively. The output of PFR-2 is mixed with the feed stream to PFR-3. As mentioned previously, initiators are introduced at the inlet of every reactor. They have a temperature of 0°C and a pressure equal to the operating pressure of the reactor. The composition of all initiator streams is kept at 80% benzoyl peroxide and 20% di-t-butyl peroxide.

PFR-4's outlet includes not only low-density polyethylene, but also some unreacted ethylene monomer. Therefore, in order to obtain a pure LDPE product, this stream is introduced into a high-pressure separator (250 bar) followed by a low-pressure separator (1 bar). At this point the per pass conversion rate is relatively low at around 15%. The unreacted monomer should consequently be recycled back into the system in order to resolve this [119]. The ethylene streams from both separators are cooled to 40°C before being sent to multi-compressors and mixed together. 95% of the unreacted monomer, having a temperature of 140°C and a pressure of 2000 bar, is recycled back into the system and blended with the feed stream. The remaining part is sent to the boiler and used as fuel to prevent accumulation. All PFRs are designed and scaled to have similar residence time as the conventional LDPE process. The final product has a flow rate of 5.82 tonnes per hour, equivalent to 77.1% overall conversion, and a mass purity of 99.92%. The total electricity demand from this unit is 9.8 MW, while the cooling demand is at 11.3 MW.

Table 4-1: Summary of the process assumptions and simulations results of the LDPE unit

Feed Conditions				
Pressure	31 bar	Temperature	-12 °C
Mass flow	7.2 tonne/h		
Composition (mass %)	C_2H_4:99.5, CH_4:0.036, C_2H_6:0.464		
Polymerization Reactor				
PFR-1 Length	139.8 m		
Residence time	31.3 s		
Operating pressure	2000 bar	Pressure drop	55.9 bar
PFR-2 Length	129.4 m		
Residence time	27.8 s		
Operating pressure	1944 bar	Pressure drop	58.8 bar
PFR-3 Length	145.4 m		
Residence time	19.1 s		
Operating pressure	1900 bar	Pressure drop	58.1 bar
PFR-4 Length	131.2 m		
Residence time	16.8 s		
Operating pressure	1842 bar	Pressure drop	59.7 bar
Overall length	545.8 m		
Diameter	0.057 m		
Residence time	95 s		

4.1.3.2. LDPE Polymerization kinetics

The polymerization of ethylene into LDPE follows a free-radical polymerization mechanism, as shown in Table 4-2. The rate constants of each reaction were obtained from [118].

Table 4-2: Free radical polymerization mechanism

Reaction type	Description	Pre-exponential rate constant (1/s)
Initiator decomposition	$I_j \rightarrow 2RI_j$	2.5×10^{14}
Chain initiation	$M + RI_j \rightarrow P_n$	5.93×10^{18}
Propagation	$P_n + M \rightarrow P_{n+1}$	2.5×10^8
Chain transfer to monomer	$P_n + M \rightarrow D_n + P_1$	2.5×10^8
Chain transfer to polymer	$P_n + D_m \rightarrow D_n + P_m$	1.24×10^6
β-scission	$P_n \rightarrow D_{n-k} + P_k$ (double bond)	6.07×10^7
Termination by disproportionation	$P_n + P_m \rightarrow D_n + D_m$ (double bond)	2.5×10^9
Termination by combination	$P_n + P_m \rightarrow D_{n+m}$	2.5×10^9
Short-chain branching	$P_n \rightarrow P_n$ (SCB)	1.3×10^9

The initiators are symbolized by I_{j1} and I_{12}, referring to benzoyl peroxide and di-t-butyl peroxide respectively, and consequently, the radicals formed from the initiator decomposition are denoted as RI_j, where j=1, 2. n, m, and k refer to the length of the polymer segment.

The main reactions involved in the free radical polymerization are initiation, propagation, and termination [119]. In the case of LDPE, two initiators are present, and therefore, the first two reactions are the decomposition of the initiators into radicals. These radicals (RI_j) are added to the monomer (M) in order to form an active segment (P), also known as a live segment or live polymer [55,120,121]. This is known as chain initiation. Propagation is when the presence of monomers and the formation of live polymers trigger a series of reactions that lead to longer polymer chains [49,120]. The final principal step is termination which can occur in two ways: termination by combination or termination by disproportionation. The former involves the addition of two active segments of similar or different lengths, to form one dead polymer [120]. The latter also entails two active polymer segments; however, two dead polymers are generated with double bonds developing at one end of each chain [55,120].

Additional side reactions that must be considered include chain transfer, β-scission, and short-chain branching, also known as back-biting [49,55,120]. Chain transfer to monomer is when an active segment and a monomer react together to give a dead polymer chain, with an unsaturated end, and a new active segment [55]. Chain transfer to polymer, on the other hand, is the reaction that takes place between an inactive polymer and an active polymer [55]. The radical at the end of the active segment is transferred intermolecularly to the dead polymer, forming a new active polymer and a new dead polymer. However, in this case, the radical is not external, but rather it is relocated to an internal position [55,120]. If monomers are further added to these active segments, long chain branching is favored [55]. For short chain branching, [49,55,120] mentioned an intramolecular transfer of radicals from the end of the chain to an internal location within the same chain; this is known as back-biting, where short chain branches are generated. β-scission is the reaction where a split occurs in a linear active polymer chain, such that two polymer chains are produced, one dead and one living with a double bond at one end [55].

4.1.4. HDPE production

4.1.4.1. Process description

There are two primary approaches for producing HDPE: Slurry polymerization, and gas-phase polymerization. Due to the presence of a solvent, slurry polymerization requires extra purification and separation units, making it more expensive than gas-phase polymerization [61]. Regardless, this approach remains dominant in the market, as it offers a number of desirable features, such as moderate process conditions, high conversion, and easy operation and heat control [62]. In addition, as mentioned by Daftaribesheli [61], the majority of catalysts that are developed for HDPE production are suitable for the slurry polymerization approach. Unlike LDPE synthesis, slurry HDPE production typically takes place in continuous stirred tank reactors (CSTR) or loop reactors in the presence of the titanium tetrachloride (TiCL$_4$) catalyst, and triethylaluminium

(TEA) co-catalyst [59]. A PFD of the process is shown in 4-6, which is based on the CX technology developed by Mitsui Chemicals [122]. The Perturbed Chain-Statistical Associated Fluid theory (PC-SAFT) was chosen as the equation of state, as is the case in other works [123,124].
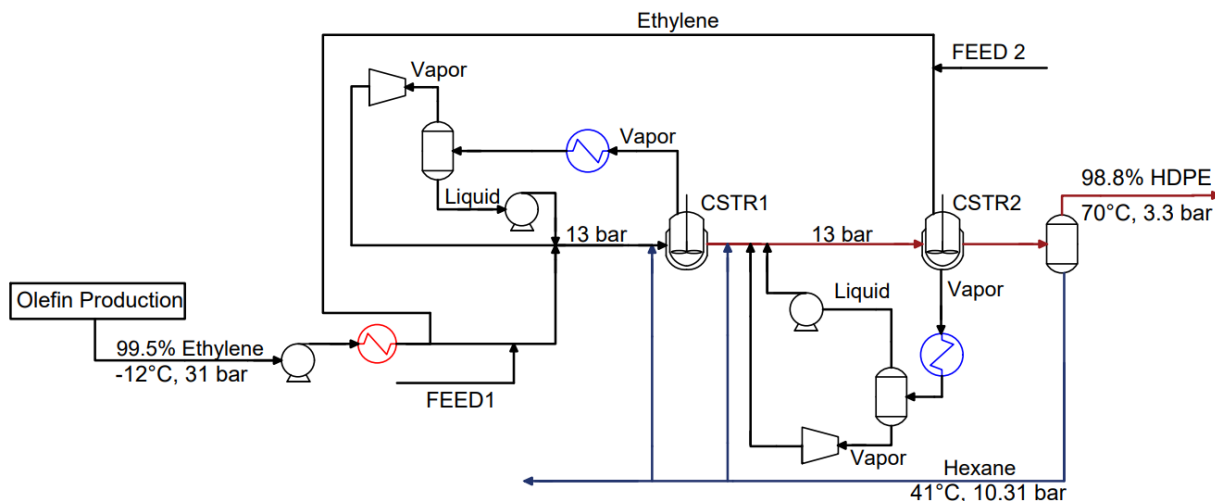
Figure 4-6: Simplified process flow diagram of HDPE slurry polymerization

Ethylene stream from the olefin production unit is compressed and heated to 45°C and 13.01 bar [124]. It is then split into two streams, 57.6% are mixed with FEED1, which consists of hexane, catalyst and co-catalyst, and hydrogen, and fed continuously into the first reactor (CSTR1), while the rest are pumped into the second reactor (CSTR2), to a pressure of 13 bar, after mixing with FEED2, hydrogen and hexane [124]. A summary of the design parameters and assumptions are listed in Table 4-3.

The liquid product (slurry) of CSTR1 is also sent to the second reactor. In order to increase the overall conversion rate, the vapor streams of both reactors are reintroduced back into the system through coolers, pressure changers and flash drums [124]. The slurry of CSTR2, which contains the polymer, is sent to a centrifugal separator, which is modeled as a component separator in Aspen Plus. The main product stream contained the polymer, while the other outlet of the separator, containing the solvent hexane and some unreacted ethylene, is sent back to both reactors [124]. The final flow rate of the polymer was 6.96 tonne/h which translates into a conversion rate of 97.6%. The electricity demand for this unit was 0.141 kW.

Table 4-3: Summary of the process assumptions and simulation results of the HDPE unit

Feed Conditions		
Feed 1 Stream	Pressure	13 bar
	Molar flow	50.6 kmol/h
	Composition (mole %)	Hexane: 90.67, H_2: 9.24, $TiCl_4$: 0.001, TEA: 0.05
Feed 2 Stream	Pressure	13 bar
	Molar flow	17.04 kmol/h
	Composition (mole %)	Hexane: 99.39, H_2: 0.61
Polymerization Reactors		
CSTR 1	Volume	25.98 m^3
	Residence time	1.7 h
	Operating pressure	80.3 bar
	Operating temperature	85 °C
CSTR 2	Volume	43.30 m^3
	Residence time	1.15 h
	Operating pressure	3.3 bar
	Operating temperature	78 °C

4.1.4.2. HDPE Polymerization kinetics

The production of HDPE from ethylene is a low-pressure process that follows a coordination polymerization mechanism [125]. The catalyst-cocatalyst pair used in the reaction are titanium tetrachloride ($TiCL_4$) and triethylaluminium (TEA), which are Ziegler-Natta catalysts. The reaction involves several components: the monomer ethylene, the catalyst and co-catalyst $TiCl_4$ and TEA, the solvent n-hexane, and the chain transfer agent hydrogen. The reaction mechanism used is from [124], and can be found in Table 4-4, and the rate constants and activation energies can be found in Tables 4-5 and 4-6, respectively.

Table 4-4: Homopolymerization of HDPE mechanism

Reaction type	Description
Activation	$CP_j + A \xrightarrow{k_{a_j}} P0_j$
Initiation	$P0_j + M \xrightarrow{k_{i_j}} P1_j$
Propagation	$Pn_j + M \xrightarrow{k_{p_j}} P_{(n+1)j}$
Chain transfer to monomer	$Pn_j + M \xrightarrow{k_{tM_j}} P1_j + Dn_j$
Chain transfer to hydrogen	$Pn_j + H_2 \xrightarrow{k_{tH_j}} P0_j + Dn_j$
Chain transfer to co-catalyst	$Pn_j + A \xrightarrow{k_{tA_j}} P0_j + Dn_j$
Chain transfer to β-hydride	$Pn_j \xrightarrow{k_{t_j}} P0_j + Dn_j$

Reaction type	Description
Deactivation	$Pn_j \xrightarrow{k_{d_j}} CD_j + Dn_j$ $P0_j \xrightarrow{k_{d_j}} CD_j$

Table 4-5: Pre-exponential rate constants in homopolymerization [126]

Rate Constants	Site 1	Site 2	Site 3	Site 4	Site 5	Units
k_a	228.131	228.131	228.131	228.131	228.131	L/(mol.s)
k_i	4562	4562	4562	4562	4562	L/(mol.s)
k_p	2816.49	6890.73	8670.46	3650.72	798.595	L/(mol.s)
k_{tM}	0.00175	0.00175	0.00175	0.00175	0.00175	L/(mol.s)
k_{tH}	354	208.5	78.6	11.8	0.778	$L^{0.5}/(mol^{0.5}.s)$
k_{aA}	0.00175	0.00175	0.00175	0.00175	0.00175	L/(mol.s)
k_t	8E-7	8E-7	8E-7	8E-7	8E-7	1/s
k_d	4E-5	4E-5	4E-5	4E-5	4E-5	1/s

Table 4-6: Activation energies in homopolymerization [126]

Activation Energy (kJ/mol)	Site 1	Site 2	Site 3	Site 4	Site 5
E_a	37.7	37.7	37.7	37.7	37.7
E_i	37.7	37.7	37.7	37.7	37.7
E_p	37.7	37.7	37.7	37.7	37.7
E_{tM}	58.6	58.6	58.6	58.6	58.6
E_{tH}	58.6	58.6	58.6	58.6	58.6
E_{aA}	58.6	58.6	58.6	58.6	58.6
E_t	58.6	58.6	58.6	58.6	58.6
E_d	0	0	0	0	0

The first step is activation, where the co-catalyst (A) reacts with the catalyst (Cp) in order to activate it [62]. This creates vacant sites, symbolized by $P0_j$, which are attached to a polymer chain, where j represents the location of the active site [124]. After activation comes initiation, where the vacant sites of the activated catalyst react with ethylene (M) to produce an activated site $P1_j$ on a polymer that has a single segment [62,124]. Propagation is the addition of monomer to the active polymer to produce a living polymer with a longer chain Pn, with n being the length of the polymer

chain [62,127]. In other words, initiation is the formation of an intermediary chain which transforms into a growing polymer chain during propagation [128].

Chain transfer (CT) occurs in four separate reactions: chain transfer to monomer, chain transfer to hydrogen, chain transfer to co-catalyst, and chain transfer to β-hydride. [62] describes chain transfer reactions as the disengagement of a living polymer segment from the catalyst to create a dead polymer chain, but also to form a new activated polymer segment. The dead polymer chain cannot partake in any other reactions, the new living segment however, can form newer and longer chains via propagation [129]. CT to monomer forms a polymer with an activated site P_{1j} with an unsaturated end, and a dead polymer of length n [62,128]. During CT to hydrogen, which is the chain transfer agent, the living polymer chain dissociates such that a hydrogen atom binds with the active catalyst and forms a vacant site $P0_j$, while the other joins the polymer segment and forms a dead polymer (Dn_j) of length n [124]. CT to co-catalyst involves a similar process to CT to H_2, however, the co-catalyst binds to the active polymer chain to form a dead polymer with an unsaturated end, while the ethyl group from the co-catalyst binds to the active site to form a vacant site $P0_j$ [124,130]. Chain transfer to β-hydride, also known as spontaneous CT or β-hydrogen elimination, is when a hydrogen atom is removed from the active polymer, forming a double bond and consequently a dead polymer, and bound to the active site forming a vacant site [128].

The last step involved in the Z-N polymerization mechanism is deactivation, where the catalytic active sites deactivate spontaneously to form dead or inactive sites [62,127]. The vacant sites generated in the CT reactions are deactivated to form dead sites, while the activated polymers transform into dead polymer chains as well as dead catalyst sites [62,124].

5. Results and discussion

5.1. Life cycle assessment

LCA is conducted based on the ISO 14040 standard, which describes the four phases of LCA: goal and scope definition, life cycle inventory analysis, life cycle impact assessment, and life cycle interpretation.

5.1.1. Goal and scope definition

The main purpose behind this work was to develop a CCU-based HDPE and LDPE production processes via the CCU-MTO pathway, evaluate the environmental impacts and energy consumption of the life cycle (cradle to gate) of LDPE and HDPE products, and compare the results to those of the conventional pathway. The boundaries for this LCA study include acquiring and processing raw materials, production and recovery of methanol, olefin production, polymer production, and electricity consumption as shown by Figure 5-1. They exclude the impacts of plant construction and equipment maintenance, additional processing, product distribution and use, and end-of-life treatments, as the study is concerned only with the emissions released from the production process. Furthermore, the emissions from initiator and catalyst production are not included in our calculations. A functional unit of 1 kg of desired product (LDPE or HDPE) is used.
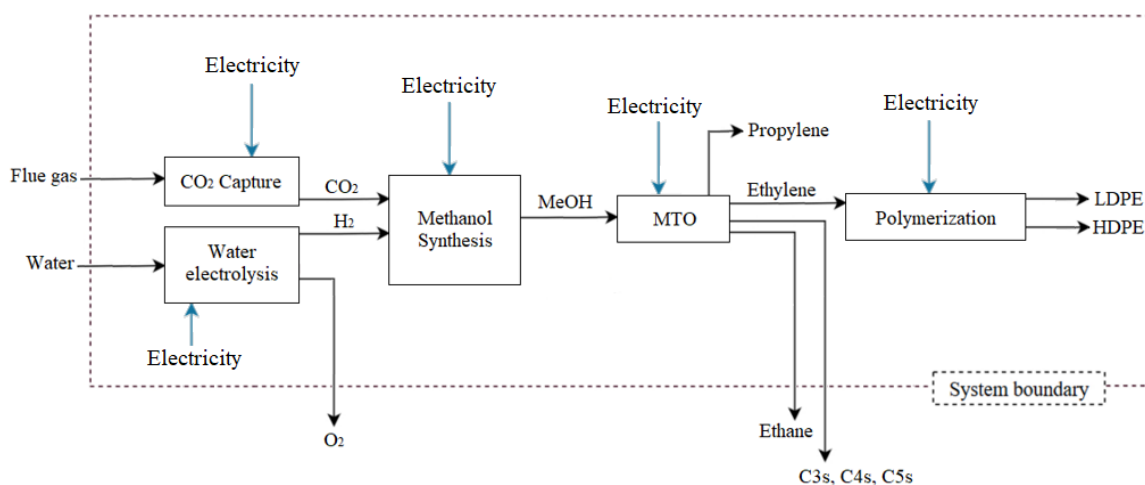
Figure 5-1: System boundary of LDPE and HDPE produced via CCU-MTO pathway

Life cycle inventory analysis

The inputs and outputs of the product systems (as stated by the ISO 14040) are determined from the simulation results of the respective processes for LDPE and HDPE production in Aspen Plus. The simulation data that led to the production of 5.81 and 6.88 tonnes/h of LDPE and HDPE, respectively, are listed in Table 5-2. In the LCA of these CCU pathways, the carbon intensity and other environmental implications of power production are among the most important factors to consider. In Canada, the electricity generation options, and respective emissions vary from one

32

province to another. To account for this diversity, three provinces, Quebec, Ontario, and Alberta, were considered. By obtaining the provincial energy profiles from [131], and the LCA results of the different electricity production methods from CIRAIG [132], the GHG emissions from each province were obtained. The results can be found in Table 5-1. Each emission translates into a different impact category when looking at the LCA. The LCI data of the conventional HDPE and LDPE production processes were taken from the Ecoinvent database and validated with published works.

Table 5-1: Main electricity generation emissions in three different Canadian provinces

Province	Quebec	Ontario	Alberta
g CO_2 eq/kWh	17.74	39.32	682.87
mg Phosphate/kWh	8.83	23.86	276.51
g 1,4-dichlorobenzne/kWh	10.16	52.46	51.31
μg CFC-11/kWh	0.80	14.85	32.52
mg ethene/kWh	3.86	9.53	131.09
g SO_2/kWh	0.05	0.15	14.40

5.1.2. Life cycle impact assessment (LCIA)

The LCA of both CCU-polymer production pathways was conducted using OpenLCA 1.10.3 software. To determine the sustainability of LDPE and HDPE production via CCU-MTO pathway two different impact assessment methods, midpoint and endpoint, were implemented. The midpoint method deals with environmental problems, such as global warming, eutrophication, respiratory effects, and resource depletion [133]. As for the endpoint method, it showcases the damage inflicted by environmental problems on three categories human health, resource depletion, and ecosystem quality [134].

The TRACI 2.1 impact assessment method was chose as the midpoint assessment method. [135]. The different impact categories were evaluated including environmental impacts such as eutrophication, acidification, global warming, ozone depletion, and fossil fuel depletion, and human health impacts such as respiratory effects. All the impact categories were expressed in terms of kg emission equivalent (eq.) apart from fossil fuel depletion which was displayed in MJ. Additionally, in order to be able to compare the overall impacts of the proposed processes with those of the conventional methods, the ReCiPe Endpoint (H,A) impact assessment method was chosen (as the endpoint assessment method), which estimates the impacts in terms of damage points per kg of product. This method mainly covers the following three categories (endpoints): ecosystem quality, human health, and resources, with numerous subcategories (Please see Appendix A.2 information for more details). Moreover, two scenarios were explored for the evaluation of the by-products in the midpoint and endpoint lifecycle assessment. In scenario 1, no credit is given for any of the by-products. However, in scenario 2, propylene, the primary by-product of our proposed pathways, is taken into account of our LCA calculations. Hence, the

avoided emissions and energy consumption associated with this by-product were included in our calculations using the ISO 14044 by-product expansion methodology. It should be noted that we did not consider the other by-products (ethane, C3s, C4s, and C5s, see Figure 4-4 and Table 5-2), mainly because those streams may need further purification in order to be marketable.

5.2. Results

The overall mass balance and a comparison of the net electricity consumption of the CCU-LDPE and HDPE pathways are illustrated in Table 5-2. It should be noted that waste streams from different units are not included in the table. Each pathway is divided into 6 process units (Figure 4-1):
- CO_2 unit: CO_2 capture and compression
- H_2 unit: Hydrogen production using PEM hydrolysis and hydrogen compression
- Methanol production: Methanol synthesis and recovery
- Olefins production: MTO synthesis, purification, and product recovery units (Figure 4-3 and Figure 4-4)
- Polymer production: LDPE or HDPE production unit (Figure 4-5 and Figure 4-6)

Table 5-2: Simulation results of CCU-LDPE and HDPE production processes

	LDPE	HDPE
Inputs (kg/h)		
CO_2	62,090	62,090
H_2	8,031	8,031
Products (kg/h)		
LDPE	5,816	-
HDPE	-	6,880
CO_2	13,960	10,474
By-products (kg/h)		
Propylene	5,076	5,076
Ethane	383	383
Propane	990	990
C4s	1,907	1,907
Gasoline	730	730
Total Electricity Demand (MW)	482.7	473

According to our simulation results, the net CO_2 utilization rate of the CCU-LDPE is 8.28 kg/kg LDPE, while it is 7.50 kg/kg HDPE. This difference is mainly due to the lower conversion of the LDPE reactor. The Sankey diagrams, which show the carbon flow in both LDPE and HDPE production pathways, are shown in Figures 5-2 and 5-3, respectively. It shows that the carbon cycle is a closed loop, where input and output are equal. In other words, carbon going into the system is equal to the carbon going out of the system, whether as hydrocarbon products, or as CO_2.
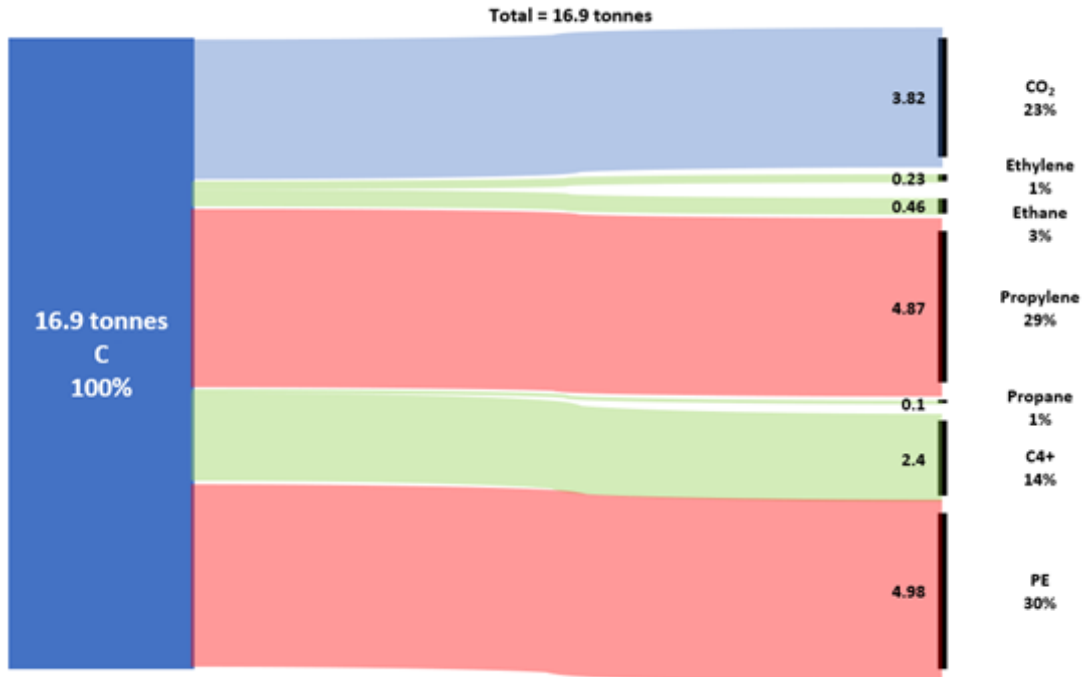
Figure 5-2:Sankey diagram of the carbon flow of the CCU-LDPE production pathway
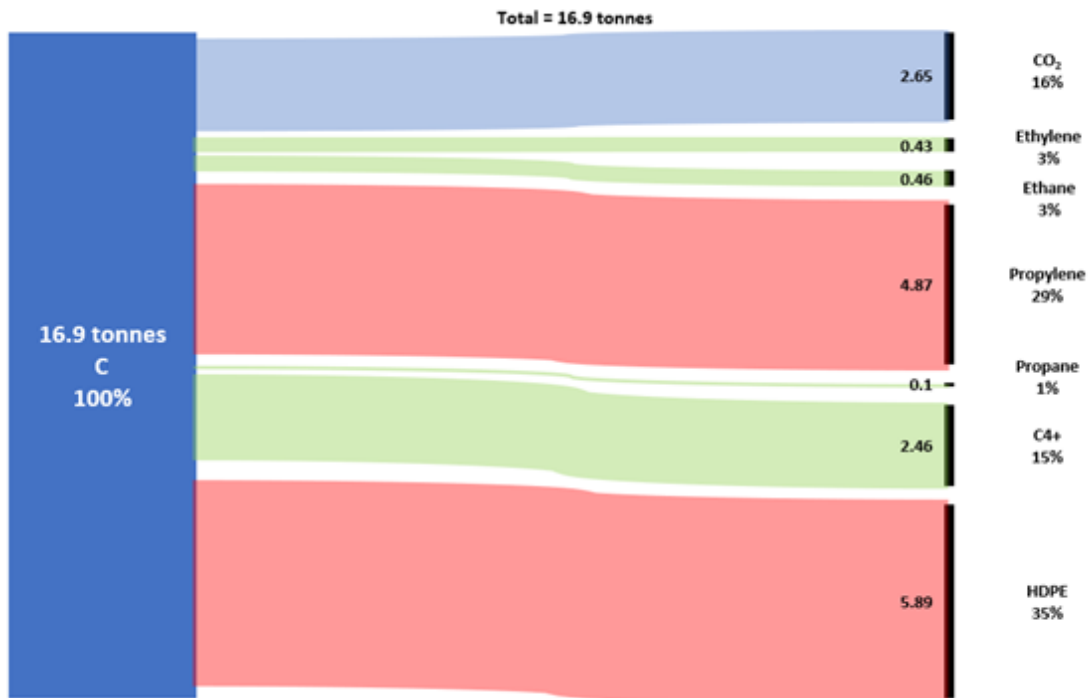
Figure 5-3: Sankey Diagram of the carbon flow of the CCU-HDPE pathway

Figures 5-2 and 5-3 show that the net CO_2 utilization rate of the proposed processes is around 77% and 84% for CCU-LDPE and CCU-HDPE, respectively, considering all products. In the proposed pathways, 30% and 35% of the inlet carbon are converted to LDPE and HDPE, respectively.

Propylene is the second important route for carbon. This by-product is the main feedstock of the Polypropylene polymer. The process simulation and analysis of this product is out of the scope of this work and will be presented in a separate article.

5.2.1. Electricity Demand

The difference in electricity demand between LDPE and HDPE is attributed to the difference in operating conditions during polymerization; where LDPE was produced under 2000 bar, HDPE had an operating pressure of 13 bar. This translates into a higher overall electricity demand for LDPE compared to HDPE. The conversion of ethylene into to LDPE requires 0.08 kWh electricity per kg LDPE, while the production of 1 kg HDPE requires 0.01 kWh of electricity. Figures 5-4 and 5-5 show a more detailed comparison of the electricity consumption of each unit. It can be seen that hydrogen production and compression are the most energy-intensive units with more than 87 and 88% of the total electricity consumption for LDPE and HDPE production, respectively. CO_2 capture and hydrogen compression are the second and third largest consumers of power.
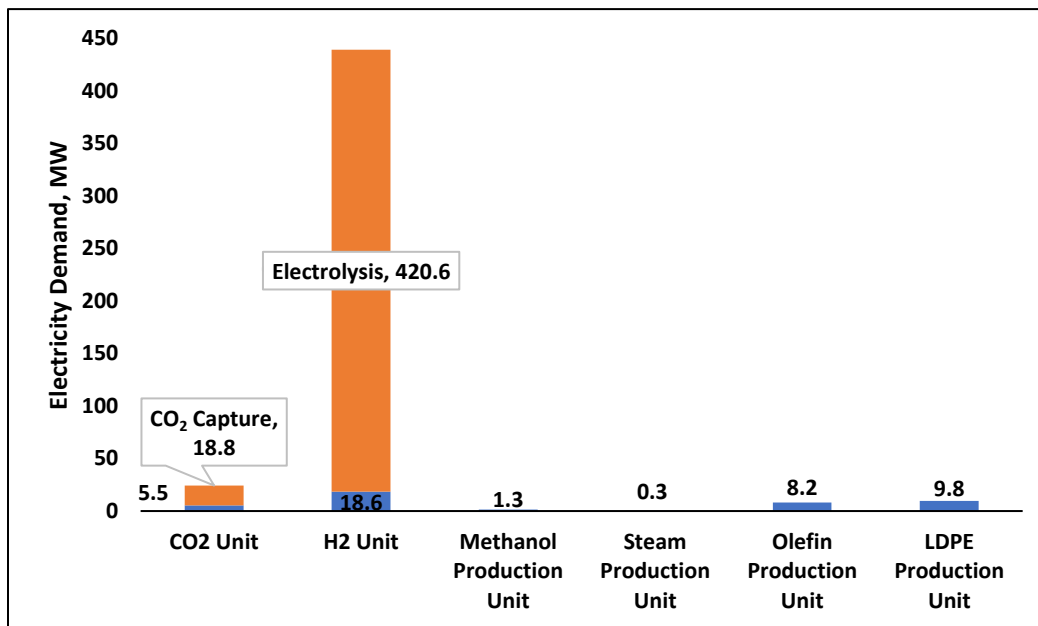
Figure 5-4: The electricity demand of the CCU-LDPE pathway
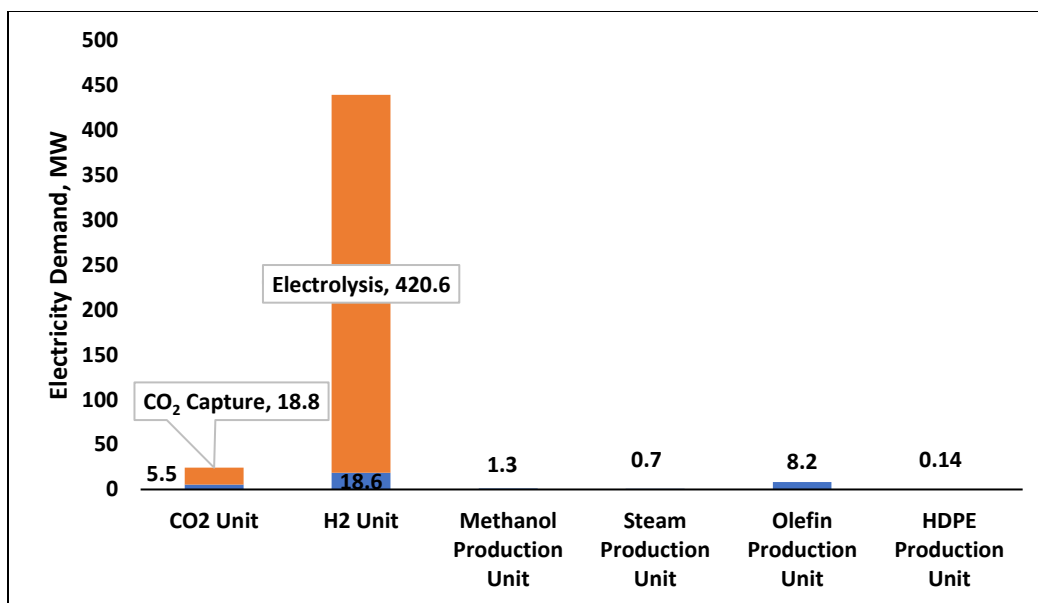
Figure 5-5: Electricity demand for CCU-HDPE pathway

5.2.2. LCA results

As mentioned previously, electricity is one of the key factors affecting the GHG emissions of the CCU pathways. Therefore, the LCA was conducted in three different Canadian provinces, Quebec, Ontario, and Alberta, to investigate the impact of the carbon intensity and other emissions of each province. Tables 5-3 and 5-4 summarize the midpoint LCA results of the CCU-LDPE and HDPE pathways, respectively, using TRACI 2.1 method, with and without considering propylene as an avoided by-product. In these tables, the LDPE and HDPE conventional refer to LDPE and HDPE produced via the steam cracking of ethane. Additional impact categories, for each assessment method, and their results can be found in Appendix A.1.

Table 5-3: The midpoint LCA results of the CCU-LDPE and comparison with the conventional process (per 1 kg LDPE)

	CCU Pathway						
Impact Category	Quebec		Ontario		Alberta		LDPE Conventional
Avoided propylene is considered?	Yes	No	Yes	No	Yes	No	
Global Warming kg CO_2 eq	-8.1	-6.8	-6.3	-5.0	47.2	48.4	1.92
Ozone Depletion kg CFC-11 eq	6.6E-8	6.7E-8	1.2E-6	1.2E-6	2.7E-6	2.7E-6	3.5E-8
Acidification kg SO_2 eq	6.8E-4	4.1E-3	8.9E-3	1.2E-2	1.2E-1	1.2E-1	6.2E-3
Eutrophication kg N eq	1.5E-3	1.7E-3	4.5E-3	4.7E-3	5.5E-2	5.5E-2	3.9E-3

	CCU Pathway						LDPE Conventional
Impact Category	Quebec		Ontario		Alberta		
Respiratory Effects kg PM2.5 eq	-2.3E-5	2.5E-4	4.8E-4	7.6E-4	7.0E-3	7.3E-3	6.7E-4
Fossil Fuel Depletion MJ surplus	-7.6	1.34	-1.8	6.6	122.1	130.5	10

Looking at Table 5-3, particularly the results of LDPE production via the CCU-pathway, it can be observed that for all impact categories, whether considering propylene as an avoided product or not, the lowest emissions were recorded by Quebec, followed by Ontario, and finally Alberta. The difference in emissions between provinces is attributed to the fact that each province releases different amounts of GHG emissions during electricity generation, as outlined by Table 5-1.

Table 4-5: Pre-exponential rate constants in homopolymerization [126]

Additionally, comparing the two scenarios mentioned in section 2.5.3, it can be seen that when propylene is considered as the avoided product, all impact values are significantly reduced, regardless in which province the production of LDPE is taking place. The most noticeable differences are in global warming and fossil fuel depletion impact categories. The decrease in emissions when the by-product is considered as an avoided product is because, as mentioned in section 2.5.3, the emissions associated with the production of propylene are avoided, when propylene credit is considered.

Comparing LDPE production via the CCU-MTO pathway to the conventional method of LDPE production, Quebec, with and without propylene credit, result in considerably lower emissions, in all impact categories. In Ontario, some impact categories recorded slightly higher values, such as ozone depletion and eutrophication. However, the difference is relatively negligible. In contrast, in Alberta, regardless of whether the impact of propylene by-product is included, production of LDPE via the CCU-pathway resulted in higher emissions in all impact categories compared to the conventional pathway.

The most impacted category is fossil fuel depletion, which as explained by [136], refers to the "additional amount of energy needed to extract one unit of fossil fuel in the future". Regardless of whether or not propylene is avoided, Alberta displays positive surplus. This is because 91% of the electricity in Alberta is dependent on fossil fuels, such as coke and natural gas, compared to the 1% in Quebec and Ontario [131]. In the latter two provinces the impact of propylene is significant on fossil fuel depletion category, such that when propylene is not included in the LCA calculations, both provinces show positive results for fossil fuel depletion. This can be explained by the fact that, while renewable electricity contributes significantly in these provinces, the power grid is not yet 100% carbon-free. The second reason is that none of the by-products are included in our calculations, and the whole load of carbon emissions has been placed on the LDPE product.

Negative fossil fuel depletion implies that no fossil fuels will be extracted in the future, and consequently, and energy will instead be saved.

Table 5-4: The midpoint LCA results of the CCU-HDPE and comparison with the conventional process (per 1 kg HDPE)

	CCU Pathway						
Impact Category	Quebec		Ontario		Alberta		HDPE Conventional
Avoided propylene is considered?	Yes	No	Yes	No	Yes	No	
Global Warming kg CO_2 eq	-7.4	-6.3	-5.9	-4.8	38.4	39.5	1.86
Ozone Depletion kg CFC-11 eq	5.5E-8	5.5E-8	1.0E-6	1.0E-6	2.2E-6	2.2E-6	4.6E-8
Acidification kg SO_2 eq	5.1E-4	3.4E-3	7.4E-3	1.0E-2	9.6E-2	9.9E-2	5.7E-3
Eutrophication kg N eq	1.3E-3	1.4E-3	3.7E-3	3.9E-3	4.5E-2	4.5E-2	2.6E-3
Respiratory Effects kg PM2.5 eq	-2.4E-5	2.1E-4	4.0E-4	6.3E-4	5.8E-3	6.1E-3	5.8E-4
Fossil Fuel Depletion MJ surplus	-6.0	1.1	-1.7	5.4	100.9	108.0	10.2

As shown in Table 5-4, similar trends can be noticed between the results of LDPE and HDPE: when considering the CCU-pathway, with and without propylene credit, Quebec shows the lowest emissions, followed by Ontario and then Alberta. The comparison of HDPE produced via CCU-MTO pathway and conventional pathway yields similar results as comparing LDPE produced from the same two pathways: production in Quebec yields lower emissions regardless of propylene considerations, HDPE production in Ontario generally yields less results than production via conventional with a few, but insignificant exceptions, and production Alberta always produces more emissions than conventional. Additionally, the emissions from polyethylene production, in all provinces, are less when propylene is considered an avoided product than when it is not.

The ReCiPe endpoint results of the CCU-LDPE and HDPE pathways in three different provinces, with and without propylene as an avoided by-product, and their comparison with those of the conventional steam cracking method are shown in Figures 5-6 and 5-7, respectively. The results are displayed in points/kg of plastic, where one point represents the damage or impact of one person per year on each of the different categories. To clarify, negative points translate to avoided impacts, while positive points refer to the extent of the damage to each of the categories.
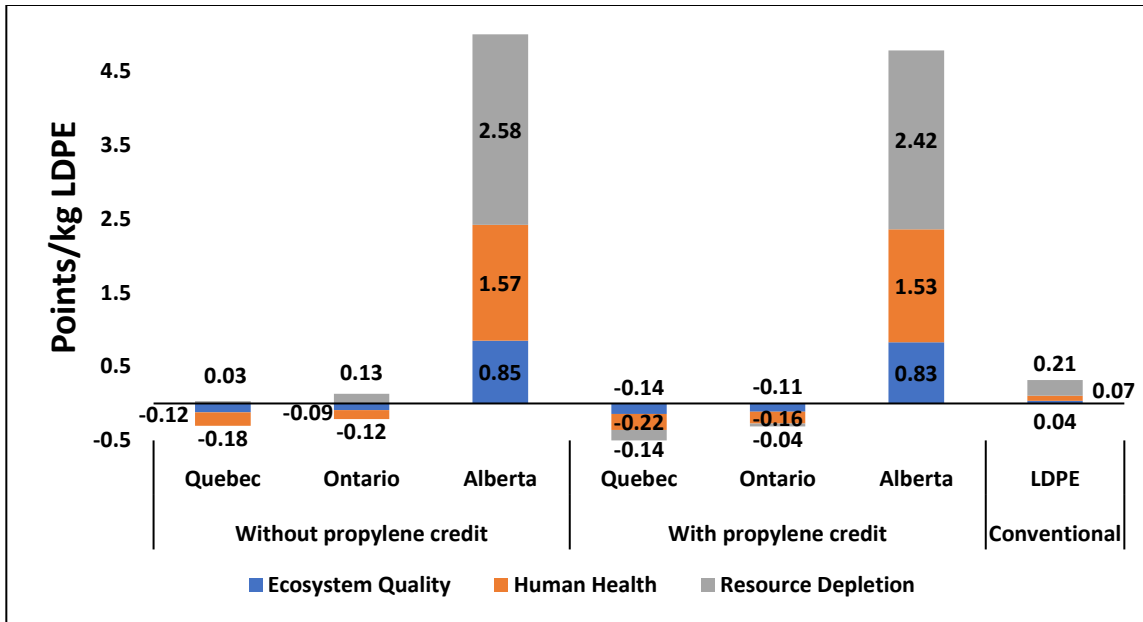
Figure 5- 6: The endpoint LCA results of the CCU-LDPE, with and without propylene credit, and comparison with the conventional process (per 1 kg LDPE)

Figure 5-6 demonstrates that, regardless of whether propylene credit is included or not, Quebec and Ontario achieve better results than Alberta and the conventional method in all aspects. Results of LDPE production in Alberta are the most comparable to those of the conventional method of LDPE production. The latter, as expected, has positive (damage) points in all three categories, resource depletion being the most impacted (66% of damages). When propylene is considered as an avoided product, Quebec and Ontario exhibit negative points in all impact categories. However, when propylene is not deemed an avoided product, these two provinces maintained negative points in two out of three impact categories (resource depletion being the exception). The negative points indicate that the production of LDPE via the CCU-MTO pathway in these two provinces does not contribute any further damage to human health and ecosystem quality. As for resource depletion, even though Quebec and Ontario exhibit positive points when propylene credit is not considered, the results are still less than Alberta and the conventional method as well. This is attributed to the insignificant dependence of these two provinces on fossil fuels for electricity compared to Alberta.

Alberta, on the other hand, inflicts additional damage in all impact categories regardless of propylene credit. The resource depletion category is the most impacted, such that it receives around 51% of the overall damage in Alberta, whether or not credit is attributed to propylene production. Compared to the conventional method, LDPE production via CCU-pathway in Alberta contributes more damage in all aspects.

Looking at the total impact with propylene credit, it can be seen that the CCU-LDPE pathway in Quebec and Ontario does not provide any damage, such that their total impact is -0.46 and -0.28 points/kg LDPE, respectively, which is significantly better than the overall result of the

conventional method that amounts to 0.32 points/kg LDPE. Alberta yields a total impact of 4.78 points/kg LDPE, which is higher than the conventional method.
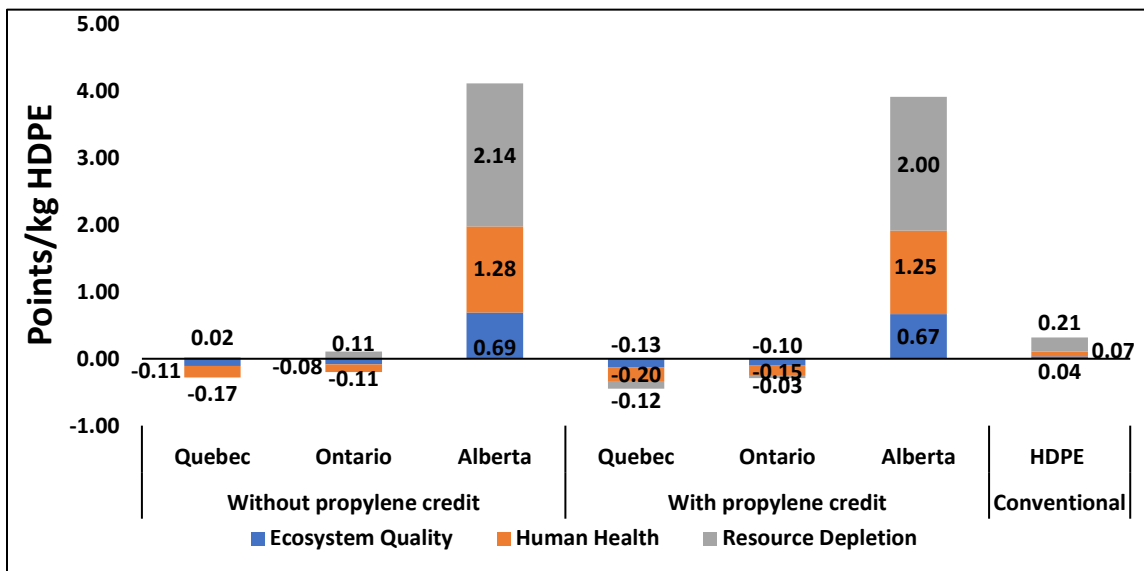
Figure 5-7: The endpoint LCA results of the CCU-HDPE and comparison with the conventional process (per 1 kg HDPE)

Figure 5-7 shows the ReCiPe Endpoint impact assessment results of high-density polyethylene. The conventional method yields damage in all categories, with resource depletion inflicting the majority of this damage. Production of HDPE in Quebec and Ontario via the CCU-MTO pathway yields better results than production in Alberta (via the same method) and better than the conventional method, in all impact categories, regardless of by-product considerations.

Comparing the CCU-pathway to the conventional method demonstrates that, similar to LDPE ReCiPe Endpoint results, Quebec and Ontario do not cause further damage in any category when propylene credit is considered, such that they display negative points. When propylene is not considered as an avoided product, production of LDPE in these two provinces inflicts damage only in one impact category: ecosystem quality. Alberta, however, has positive damage points in all categories, regardless of propylene considerations. Also, it should be noted that Alberta has a much higher overall impact when the CCU pathway is incorporated, compared to the conventional method: 4.17 points/ kg HDPE when propylene credit is not considered, and 3.89 points/kg HDPE when it is.

5.2.3. Impact of methanol production process

Besides the CCU-MTO option, it is important to understand the impact of incorporating other methanol production pathways on the lifecycle emissions of the MTO-based LDPE and HDPE products. Hence, in this section, we incorporated the simulation results of the two other methanol production processes: 1) conventional methanol production using natural gas reforming and then the conversion of syngas to methanol, and finally methanol to olefins (NG-MTO). 2) Modification

of the reforming section by incorporating the Tri-reforming technology of natural gas for methanol production (TRM-MTO). The main difference of these are in the methanol production section. While in the CCU-MTO pathway, methanol is produced through the direct hydrogenation of CO_2 in the methanol reactor, the TRM technology is based on the reforming of natural gas using both steam and CO_2 reforming agents, and then sending the syngas to the methanol reactor. The energy consumption and emissions of the methanol production for the NG-MTO and TRM-MTO technologies are adopted from our previous work [105]. Figures 5-8 and 5-9 display the lifecycle GHG emission results of LDPE and HDPE produced via the CCU-MTO, TRM-MTO, and NG-MTO pathways (all with considering propylene as the avoided by-product).
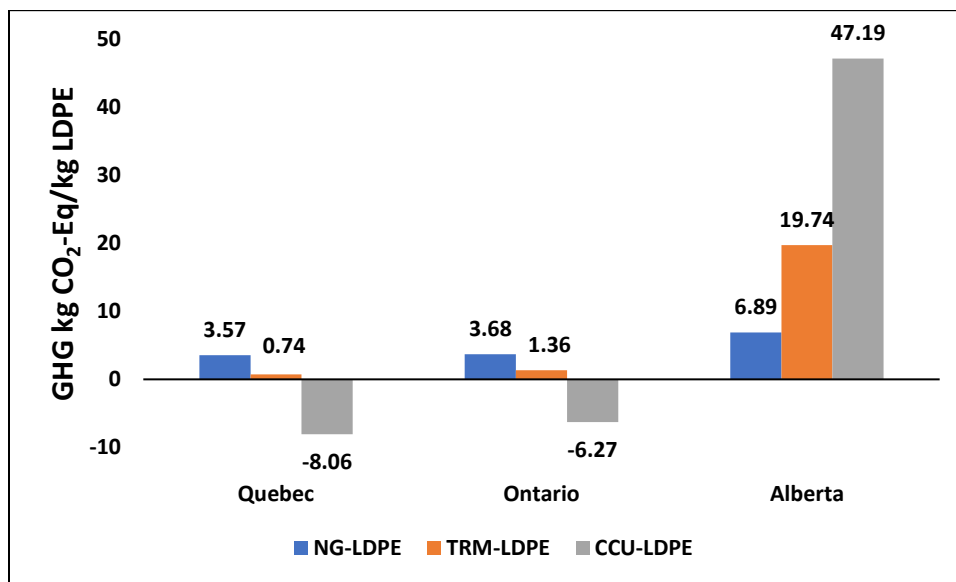
Figure 5-8: Life cycle GHG emissions of LDPE production using different methanol production pathways

Figure 5-8 shows that for the production of LDPE in Quebec and Ontario, the CCU-MTO pathway emits the least amount of GHGs compared to TRM- and NG-MTO. Out of the latter two, TRM-pathway emits less GHGs for the production of LDPE compared to NG-pathway. Out of these three pathways, only NG-LDPE emits almost 100% more CO_2 than conventional method (1.92 kg CO_2/kg LDPE) in both provinces. TRM-LDPE releases 62% and 30% less CO_2 than the conventional method for LDPE in production in Quebec and Ontario respectively. As for Alberta, the CCU-LDPE pathway contributes to the most emissions out of the three pathways, followed by TRM- and NG- pathways respectively. In Alberta, compared to the conventional method of LDPE production, all production pathways emit more emissions. This is because in the other two provinces, electricity is almost completely carbon-free. These results are comparable to those portrayed by [105].
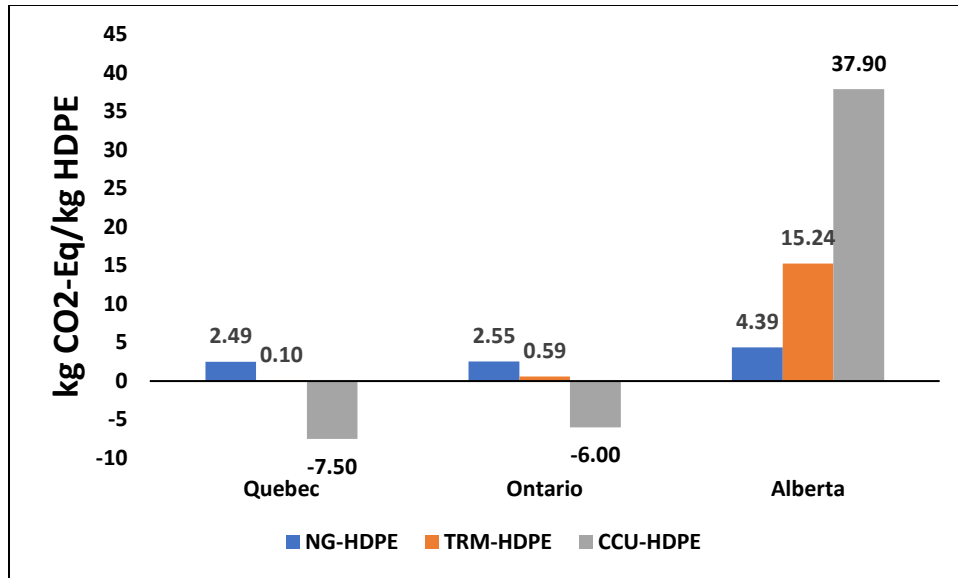
Figure 5-9: Life cycle GHG emissions of HDPE production using different methanol production pathways

Similar results to LDPE are obtained with HDPE, with less emissions in all pathways, as HDPE production requires less energy than LDPE production. The conventional method of HDPE production emits 1.86 kg CO_2/kg HDPE. Therefore, in Quebec and Ontario, the least emissions are released via the CCU-HDPE pathway, followed by TRM-HDPE, then the conventional pathway, and finally, NG-HDPE which emits around 23 and 27% more CO_2 than the conventional method in Quebec and Ontario, respectively. In Alberta, however, the conventional method produces the least amount of CO_2/kg product, followed by the NG-pathway, then TRM, and finally the CCU-MTO pathway.

6. Conclusion

The main purpose of this work was to develop and analyze carbon-negative polymer production processes to decarbonize the plastic industry, as one of the most carbon-intensive chemical sectors. The process simulation of the production of LDPE and HDPE by the CCU-MTO pathway was conducted and results were utilized for the comparative life cycle assessment of each pathway. The LCA results are used to determine whether the proposed pathways reduce the carbon footprint compared to the conventional method of production i.e., steam cracking. The simulation involved several processes, mainly CO_2 capture, water electrolysis, methanol synthesis, olefin production, and lastly, polymerization. The only difference between LDPE and HDPE production processes was in the polymerization technique. This led to variations in electricity demand such that synthesis of low-density polyethylene required around 9.7 MW more electricity than HDPE production. Consequently, the emissions from LDPE are greater than those from HDPE.

Life cycle results following both midpoint and endpoint assessment methods revealed that the CCU-MTO pathway for polymer manufacture emits less emissions in provinces like Quebec and Ontario, than the conventional method of production. According to our results, negative life cycle GHG emissions are achievable in both provinces. Compared to the conventional LDPE and HDPE processes, the CCU-LDPE pathway offers a GHG emission saving of up to 10 kg CO_2/kg LDPE (in Quebec, considering propylene as the avoided product).

On the other hand, the production of LDPE and HDPE in Alberta leads to significantly more emissions than production via the conventional method. To further verify the significance of the CCU-pathway for polymer production, it was compared to other methanol production pathways, the conventional methanol production using natural gas (NG), and the Tri-reforming of methane (TRM). The results showed that the CCU pathway yields the least carbon dioxide emissions out of these three pathways, but only in Quebec and Ontario. In Alberta, the CCU-polymer pathway proved to be the worst. This brings us to conclude that in provinces were electricity generation is dependent on fossil fuels (such as Alberta), polyethylene production via the CCU-pathway is not a viable option. Additionally, the negative CO_2 emissions suggest that the polymerization of ethylene can be used for CO_2 mitigation. In order to validate the economic efficiency of these techniques, a techno-economic analysis must be conducted, which is the subject of our future research.

Appendices

A. LCA results

A.1. TRACI 2.1 results

Tables A-1 and A-2 display additional impact categories from the TRACI 2.1 impact assessment method for LDPE and HDPE production via CCU-pathway respectively, with and without propylene credit, and compared to the conventional method of production.

Table A-1: The midpoint LCA results of the CCU-LDPE and comparison with the conventional process (per 1 kg LDPE)

Impact Category	CCU Pathway						LDPE Conventional
	Quebec		Ontario		Alberta		
Avoided propylene is considered?	Yes	No	Yes	No	Yes	No	
Smog kg O_3 Eq	-0.04	2.9E-3	-0.04	7.1E-3	0.05	9.8E-2	0.09
Ecotoxicity CTUe	2.48	3.8	18.32	19.65	17.89	19.22	18.22
Carcinogenics CTUh	2.4E-7	2.6E-7	1.3E-6	1.3E-6	1.3E-6	1.3E-6	1.3E-7
Non-carcinogenics CTUh	6.5E-8	7.7E-8	3.9E-7	4E-7	3.8E-7	3.9E-7	2.6E-7

Table A-2: The midpoint LCA results of the CCU-HDPE and comparison with the conventional process (per 1 kg HDPE)

Impact Category	CCU Pathway						HDPE Conventional
	Quebec		Ontario		Alberta		
Avoided propylene is considered?	Yes	No	Yes	No	Yes	No	
Smog kg O_3 Eq	-0.04	3.4E-4	-0.04	8.4E-4	-0.03	1.2E-2	0.08
Ecotoxicity CTUe	-0.66	0.45	1.20	2.31	1.15	2.26	16.32
Carcinogenics CTUh	1.2E-8	3.0E-8	1.4E-7	1.6E-7	1.4E-7	1.5E-7	1.4E-7
Non-carcinogenics CTUh	-9.3E-10	9.1E-9	3.7E-8	4.7E-8	3.6E-8	4.6E-8	2E-7

Tables A.1 and A.2 display additional impact categories to those in Table 5-3 and 5-4 respectively. Similar trends can be seen, such that production of LDPE in all three provinces via the CCU-pathway shows less emissions when propylene credit is considered. Additionally

Quebec shows the least amount of emissions, followed by Ontario, Alberta, and finally the conventional method, regardless of propylene consideration.

A.2. ReCiPe (H,A) results

Tables A-3 and A-4 display the subcategories of the three main impact categories from the ReCiPe (H,A) impact assessment method for LDPE and HDPE production via CCU-pathway respectively, with and without propylene credit, and compared to the conventional method of production.

Table A-3: The endpoint LCA results of the CCU-LDPE and comparison with the conventional process (per 1 kg LDPE)

| Impact Category | CCU Pathway | | | | | | LDPE Conventional |
| | Quebec | | Ontario | | Alberta | | |
Avoided propylene is considered?	Yes	No	Yes	No	Yes	No	
Ecosystem Quality (total) Points	**-0.14**	**-0.12**	**-0.11**	**-0.09**	**0.83**	**0.85**	**0.04**
Climate Change	-0.14	-0.12	-0.11	-0.09	0.83	0.85	0.04
Freshwater Eutrophication	2.3E-05	2.4E-05	6.5E-05	6.6E-05	7.6E-04	7.6E-04	3E-5
Terrestrial Acidification	1.2E-05	5.3E-05	1.2E-04	1.6E-04	1.5E-03	1.5E-03	6.7E-5
Human Health (total) Points	**-0.22**	**-0.18**	**-0.16**	**-0.12**	**1.53**	**1.57**	**0.03**
Climate Change	-0.22	-0.19	-0.17	-0.14	1.31	1.34	0.05
Human Toxicity	-1.1E-4	6E-8	-1.1E-4	1.1E-6	-1.1E-4	2.4E-6	3.5E-3
Ozone Depletion	2.3E-6	2.3E-6	4.3E-5	4.3E-5	9.4E-5	9.4E-5	2E-6
Particulate Matter Formation	-8.5E-4	5.3E-3	9.9E-3	1.6E-2	0.15	1.6E-1	1.1E-2
Photochemical Oxidant Formation	1.3E-3	2.6E-3	6.5E-3	7.8E-3	7.4E-2	7.5E-2	1.6E-3
Resources (total) Points	**0.10**	**0.27**	**-0.04**	**0.13**	**2.42**	**2.58**	**0.21**
Fossil Depletion	0.10	0.27	-0.04	0.13	2.42	2.58	0.21

Table A-4: The endpoint LCA results of the CCU-HDPE and comparison with the conventional process (per 1 kg HDPE)

Impact Category	CCU Pathway						HDPE Conventional
	Quebec		Ontario		Alberta		
Avoided propylene is considered?	Yes	No	Yes	No	Yes	No	
Ecosystem Quality (total) Points	**-0.13**	**-0.11**	**-0.10**	**-0.08**	**0.67**	**0.69**	**0.04**
Climate Change	-0.13	-0.11	-0.10	-0.08	0.67	0.69	0.03
Freshwater Eutrophication	1.9E-5	2.0E-5	5.4E-5	5.4E-5	6.3E-4	6.3E-4	4.8E-05
Terrestrial Acidification	9.6E-6	4.4E-5	9.8E-5	1.3E-4	1.2E-3	1.3E-3	7.2E-05
Human Health (total) Points	**-0.20**	**-0.17**	**-0.15**	**-0.11**	**1.25**	**1.28**	**0.07**
Climate Change	-0.20	-0.17	-0.16	-0.13	1.06	1.09	0.05
Human Toxicity	-9.3E-5	5E-8	-9.2E-5	9.2E-7	-9.1E-5	2.0E-6	5.1E-03
Ozone Depletion	1.9E-6	1.9E-6	3.6E-5	3.6E-5	7.8E-5	7.8E-5	1.6E-06
Particulate Matter Formation	-8.1E-4	4.4E-3	8.1E-3	1.3E-2	1.2E-1	1.3E-1	1.1E-02
Photochemical Oxidant Formation	1E-3	2.1E-3	5.3E-3	6.4E-3	6.1E-2	6.2E-2	1.5E-03
Resources (total) Points	**-1.2E-1**	**2.2E-2**	**-3.3E-2**	**0.11**	**2**	**2.1**	**0.21**
Fossil Depletion	-1.2E-1	2.2E-2	-3.2E-2	0.11	2	2.1	0.21

Looking at Tables A-3 and A-4, it can be seen that the subcategories of each of the impact categories, ecosystem quality, human health, and resources, follow similar trends: Regardless of whether propylene credit is considered, LDPE produced via the CCU-pathway in Quebec or Ontario achieved less points than polymers produced in Alberta or the conventional method in all aspects.

Additionally, production of LDPE in all three provinces leads to less damage in all subcategories when propylene credit is considered.

References

[1]   S. Fawzy, A.I. Osman, J. Doran, D.W. Rooney, Strategies for mitigation of climate change: a review, Environ Chem Lett. 18 (2020) 2069–2094. https://doi.org/10.1007/s10311-020-01059-w.

[2]   Rebecca Lindsey, Climate Change: Atmospheric Carbon Dioxide, National OCeanic and Atmospheric Adminstration (NOAA). (2020). https://www.climate.gov/news-features/understanding-climate/climate-change-atmospheric-carbon-dioxide (accessed May 28, 2022).

[3]   Trevor M. Letcher, ed., Climate Change, 3rd ed., Elsevier, 2021. https://doi.org/10.1016/C2019-0-01498-7.

[4]   M. Denchak, Are the Effects of Global Warming Really that Bad?, NRDC. (2016). https://www.nrdc.org/stories/are-effects-global-warming-really-bad (accessed May 21, 2022).

[5]   A.L. Radu, M.A. Scrieciu, D.M. Caracota, Carbon Footprint Analysis: Towards a Projects Evaluation Model for Promoting Sustainable Development, Procedia Economics and Finance. 6 (2013) 353–363. https://doi.org/10.1016/S2212-5671(13)00149-4.

[6]   IPCC, Global Warming of 1.5°C.An IPCC Special Report on the impacts of global warming of 1.5°C above pre-industrial levels and related global greenhouse gas emission pathways, in the context of strengthening the global response to the threat of climate change, sustainable development, and efforts to eradicate poverty, IPCC, 2018.

[7]   United Nations, Paris Agreement, (2015). https://unfccc.int/sites/default/files/english_paris_agreement.pdf (accessed May 19, 2022).

[8]   United Nations Environment Programme, The emissions gap report 2021: The Heat Is On – A World of Climate Promises Not Yet Delivered., Nairobi, 2021.

[9]   E. Bush, E. Watson, J. Fyfe, F. Vogel, N. Swart, N. Gillett, Understanding Observed Global Climate Change; Chapter 2 in Canada's Changing Climate Report, ; Government of Canada, Ottawa, Ontario, 2019. https://doi.org/10.4095/314614.

[10]   M. Denchak, J. Turrentine, Global Climate Change: What You Need to Know, (2021).

[11]   NASA, Global Warming, (2010). https://earthobservatory.nasa.gov/features/GlobalWarming/page4.php (accessed May 21, 2022).

[12]   G. Hansen, D. Stone, Assessing the observed impact of anthropogenic climate change, Nature Clim Change. 6 (2016) 532–537. https://doi.org/10.1038/nclimate2896.

[13]   IEA, Global Energy Review: CO2 Emissions in 2021, International Energy Agency, 2021.

[14]   IEA, Global Energy Review 2021, International Energy Agency, 2021.

[15]   H. Ritchie, M. Roser, Plastic Pollution, Our World in Data. (2018). https://ourworldindata.org/plastic-pollution (accessed January 10, 2022).

[16]   Ian Tiseo, • Share of global CO2 emissions by sector 2020 | Statista, Statista. (2022). https://www.statista.com/statistics/1129656/global-share-of-co2-emissions-from-fossil-fuel-and-cement/ (accessed May 31, 2022).

[17]   L. Pires da Mata Costa, D. Micheline Vaz de Miranda, A.C. Couto de Oliveira, L. Falcon, M. Stella Silva Pimenta, I. Guilherme Bessa, S. Juarez Wouters, M.H.S. Andrade, J.C. Pinto, Capture and Reuse of Carbon Dioxide (CO2) for a Plastics Circular Economy: A Review, Processes. 9 (2021) 759. https://doi.org/10.3390/pr9050759.

[18]   K. Kuusela, CARBON FOOTPRINT OF CO2-BASED POLYPROPYLENE VIA METHANOL-TO-OLEFINS ROUTE, (2020) 74.

[19]   O. Nkwachukwu, C. Chima, A. Ikenna, L. Albert, Focus on potential environmental issues on plastic world towards a sustainable plastic recycling in developing countries, Int J Ind Chem. 4 (2013) 34. https://doi.org/10.1186/2228-5547-4-34.

[20]   P. Dauvergne, Why is the global governance of plastic failing the oceans?, Global Environmental Change. 51 (2018) 22–31. https://doi.org/10.1016/j.gloenvcha.2018.05.002.

[21]   J. Zheng, S. Suh, Strategies to reduce the global carbon footprint of plastics, Nat. Clim. Chang. 9 (2019) 374–378. https://doi.org/10.1038/s41558-019-0459-z.

[22]   Ian Tiseo, Global plastic production 1950-2020, Statista. (2022). https://www.statista.com/statistics/282732/global-production-of-plastics-since-1950/ (accessed January 25, 2022).

[23]   The Ellen MacArthur Foundation, The New Plastics Economy—Rethinking the Future of Plastics, (2017).

[24]   Plastic & Climate: The Hidden Costs of a Plastic Planet, Center for International Environmental Law (CIEL), 2019. https://www.ciel.org/reports/plastic-health-the-hidden-costs-of-a-plastic-planet-may-2019/ (accessed May 31, 2022).

[25]   R.K. Sinha, N.D. Chaturvedi, A review on carbon emission reduction in industries and planning emission limits, Renewable and Sustainable Energy Reviews. 114 (2019) 109304. https://doi.org/10.1016/j.rser.2019.109304.

[26]   A. Peacock, Handbook of Polyethylene: Structures: Properties, and Applications, 0 ed., CRC Press, 2000. https://doi.org/10.1201/9781482295467.

[27] C.B. Crawford, B. Quinn, Physiochemical properties and degradation, in: Microplastic Pollutants, Elsevier, 2017: pp. 57–100. https://doi.org/10.1016/B978-0-12-809406-8.00004-9.

[28] I. Baker, Fifty Materials That Make the World, Springer International Publishing, Cham, 2018. https://doi.org/10.1007/978-3-319-78766-4_31.

[29] A.B. Strong, Plastics : materials and processing, Upper Saddle River, NJ : Pearson Prentice Hall, 2006., 2006. https://concordiauniversity.on.worldcat.org/search/detail/58451777?queryString=Plastics%3A%20Materials%20and%20processing&databaseList= (accessed June 21, 2022).

[30] I.D. Burdett, R.S. Eisinger, Handbook of Industrial Polyethylene and Technology: Definitive Guide to Manufacturing, Properties, Processing, Applications and Markets, John Wiley & Sons, Inc., Hoboken, NJ, USA, 2017. https://doi.org/10.1002/9781119159797.

[31] J.B.P. Soares, T.F.L. McKenna, Polyolefin Reaction Engineering, 1st ed., Wiley, 2012. https://doi.org/10.1002/9783527646944.

[32] R.M. Patel, Polyethylene, in: John R. Wagner, Jr. (Ed.), Multilayer Flexible Packaging, 2nd ed., Elsevier, 2016: pp. 17–34. https://doi.org/10.1016/B978-0-323-37100-1.00002-8.

[33] P. Guo, Y. Xu, M. Lu, S. Zhang, High Melt Strength Polypropylene with Wide Molecular Weight Distribution Used as Basic Resin for Expanded Polypropylene Beads, Ind. Eng. Chem. Res. 54 (2015) 217–225. https://doi.org/10.1021/ie503503k.

[34] T. Okamura, Polyethylene (PE; Low Density and High Density), in: S. Kobayashi, K. Müllen (Eds.), Encyclopedia of Polymeric Nanomaterials, Springer Berlin Heidelberg, Berlin, Heidelberg, 2015: pp. 1826–1829. https://doi.org/10.1007/978-3-642-29648-2_252.

[35] G. Wypych, Handbook of Polymers, Elsevier, 2016. https://doi.org/10.1016/C2015-0-01462-9.

[36] A.-M.M. Baker, J. Mead, Thermoplastics, in: C.A. Harper (Ed.), Modern Plastics Handbook, McGraw-Hill Education, 2000. https://www.accessengineeringlibrary.com/content/book/9780070267145/chapter/chapter1 (accessed June 24, 2022).

[37] H.V. Pechmann, Ueber Diazomethan, Ber. Dtsch. Chem. Ges. 27 (1894) 1888–1891. https://doi.org/10.1002/cber.189402702141.

[38] E. Bamberger, F. Tschirner, Ueber die Einwirkung von Diazomethan auf β-Arylhydroxylamine, Berichte Der Deutschen Chemischen Gesellschaft. 33 (1900) 955–959. https://doi.org/10.1002/cber.190003301166.

[39]   M.E.P. Friedrich, C.S. Marvel, THE REACTION BETWEEN ALKALI METAL ALKYLS AND QUATERNARY ARSONIUM COMPOUNDS, J. Am. Chem. Soc. 52 (1930) 376–384. https://doi.org/10.1021/ja01364a056.

[40]   C. Dobbin, An Industrial Chronology of Polyethylene, in: M.A. Spalding, A.M. Chatterjee (Eds.), Handbook of Industrial Polyethylene and Technology: Definitive Guide to Manufacturing, Properties, Processing, Applications and Markets, John Wiley & Sons, Inc., Hoboken, NJ, USA, 2017. https://doi.org/10.1002/9781119159797.

[41]   M. Demirors, The History of Polyethylene, in: E.T. Strom, S.C. Rasmussen (Eds.), ACS Symposium Series, American Chemical Society, Washington, DC, 2011: pp. 115–145. https://doi.org/10.1021/bk-2011-1080.ch009.

[42]   E.W. Fawcett, R.O. Gibson, J.G. Paton, M.W. Perrin, E.G. Williams, Process for the production of semi-solid and solid polymers of ethylene, DE836711C, 1952. https://patents.google.com/patent/DE836711C/en#patentCitations (accessed June 10, 2022).

[43]   Improvements in or relating to the polymerisation of ethylene, GB471590A, 1937. https://patents.google.com/patent/GB471590A/en (accessed June 25, 2021).

[44]   T.E. Nowlin, Business and Technology of the Global Polyethylene Industry: An In-Depth Look at the History, Technology, Catalysts, and Modern Commercial Manufacture of Polyethylene and its Products, John Wiley & Sons, Inc., Hoboken, NJ, USA, 2014. https://doi.org/10.1002/9781118946039.

[45]   H.R. Sailors, J.P. Hogan, History of Polyolefins, Journal of Macromolecular Science: Part A - Chemistry. 15 (1981) 1377–1402. https://doi.org/10.1080/00222338108056789.

[46]   M.A. Spalding, A.M. Chatterjee, eds., Handbook of industrial polyethylene and technology: definitive guide to manufacturing, properties, processing, applications and markets, John Wiley & Sons, Hoboken, NJ, 2017.

[47]   S. Ronca, Polyethylene, in: M. Gilbert (Ed.), Brydson's Plastics Materials, 8th ed., Butterworth-Heinemann, 2017: pp. 247–278. https://doi.org/10.1016/B978-0-323-35824-8.00010-4.

[48]   A.E. Hamielec, J.B.P. Soares, Polymerization reaction engineering — Metallocene catalysts, Progress in Polymer Science. 21 (1996) 651–706. https://doi.org/10.1016/0079-6700(96)00001-9.

[49]   D.B. Malpass, Introduction to Industrial Polyethylene_ Properties, Catalysts, and Processes, John Wiley & Sons, Inc., Hoboken, NJ, USA, 2010. https://doi.org/10.1002/9780470900468.

[50] Y.V. Kissin, Catalysts for the Manufacture of Polyethylene, in: M.A. Spalding, A.M. Chatterjee (Eds.), Handbook of Industrial Polyethylene and Technology, John Wiley & Sons, Inc., Hoboken, NJ, USA, 2017: pp. 25–60. https://doi.org/10.1002/9781119159797.ch2.

[51] O. Olabisi, Polyolefins, in: Handbook of Thermoplastics, 2006.

[52] S.X. Zhang, N.K. Read, W.H. Ray, Runaway phenomena in low-density polyethylene autoclave reactors, AIChE J. 42 (1996) 2911–2925. https://doi.org/10.1002/aic.690421019.

[53] Intratec, LDPE Production from Ethylene (High-pressure Autoclave Process) - Advanced Cost Analysis - LDPE E12A, Intratec Solutions, LLC, 2021. https://www.intratec.us/analysis/ldpe-production-cost.

[54] I.D. Burdett, R.S. Eisinger, Ethylene Polymerization Processes and Manufacture of Polyethylene, in: M.A. Spalding, A.M. Chatterjee (Eds.), Handbook of Industrial Polyethylene and Technology, John Wiley & Sons, Inc., Hoboken, NJ, USA, 2017: pp. 61–103. https://doi.org/10.1002/9781119159797.ch3.

[55] M. Häfele, Modelling and Analysis of a Production Plant for Low Density Polyethylene, (2006) 160.

[56] LyondellBasell, Licensed polyolefin technologies and Services: Lupotech, n.d.

[57] J.G. Speight, Handbook of Petrochemical Processes, 1st ed., CRC Press, Boca Raton, FL : CRC Press/Taylor & Francis Group, [2019] | Series: Chemical industries, 2019. https://doi.org/10.1201/9780429155611.

[58] UNIPOL^{TM} PE Process, (n.d.). https://www.prod.univation.com/en-us/unipol/process.html (accessed June 26, 2022).

[59] D. Wang, G. Yang, F. Guo, J. Wang, Y. Jiang, Progress in Technology and Catalysts for Continuous Stirred Tank Reactor Type Slurry Phase Polyethylene Processes, Pet. Chem. 58 (2018) 264–273. https://doi.org/10.1134/S0965544118030064.

[60] Polyethylene Technology, Chevron Phillips Chemical. (n.d.). https://www.cpchem.com/what-we-do/licensing/polyethylene-technology (accessed July 6, 2022).

[61] M. Daftaribesheli, Comparison of catalytic ethylene polymerization in slurry and gas phase, PhD, University of Twente, 2009. https://doi.org/10.3990/1.9789036528382.

[62] N.P. Khare, K.C. Seavey, Y.A. Liu, S. Ramanathan, S. Lingard, C.-C. Chen, Steady-State and Dynamic Modeling of Commercial Slurry High-Density Polyethylene (HDPE) Processes, Ind. Eng. Chem. Res. 41 (2002) 5601–5618. https://doi.org/10.1021/ie020451n.

[63] R. Geyer, J.R. Jambeck, K.L. Law, Production, use, and fate of all plastics ever made, Sci. Adv. 3 (2017) e1700782. https://doi.org/10.1126/sciadv.1700782.

[64] P.S. Chum, K.W. Swogger, Olefin polymer technologies—History and recent progress at The Dow Chemical Company, Progress in Polymer Science. 33 (2008) 797–819. https://doi.org/10.1016/j.progpolymsci.2008.05.003.

[65] K.N. Rao, A. Abdullah, Aspen HYSYS Simulation of Suspension (Slurry) Process for the Production of Polyethylene, (2018) 5.

[66] E. Castro-Aguirre, F. Iñiguez-Franco, H. Samsudin, X. Fang, R. Auras, Poly(lactic acid)—Mass production, processing, industrial applications, and end of life, Advanced Drug Delivery Reviews. 107 (2016) 333–366. https://doi.org/10.1016/j.addr.2016.03.010.

[67] T.A. Hottle, M.M. Bilec, A.E. Landis, Sustainability assessments of bio-based polymers, Polymer Degradation and Stability. 98 (2013) 1898–1907. https://doi.org/10.1016/j.polymdegradstab.2013.06.016.

[68] P.T. Benavides, U. Lee, O. Zarè-Mehrjerdi, Life cycle greenhouse gas emissions and energy use of polylactic acid, bio-derived polyethylene, and fossil-derived polyethylene, Journal of Cleaner Production. 277 (2020) 124010. https://doi.org/10.1016/j.jclepro.2020.124010.

[69] Franklin Associates, Cradle-to-Gate Life Cycle Analysis of Low-Density Polyethylene (LDPE) Resin, American Chemistry Council (ACC), Plastics Division, 2020. https://www.americanchemistry.com/better-policy-regulation/plastics/resources/cradle-to-gate-life-cycle-analysis-of-low-density-polyethylene-ldpe-resin (accessed June 14, 2022).

[70] Franklin Associates, Cradle-to-Gate Life Cycle Analysis of High-Density Polyethylene (HDPE) Resin, American Chemistry Council (ACC), Plastics Division, 2020. https://www.americanchemistry.com/better-policy-regulation/plastics/resources/cradle-to-gate-life-cycle-analysis-of-high-density-polyethylene-hdpe-resin (accessed June 14, 2022).

[71] R.A. Sheldon, M. Norton, Green chemistry and the plastic pollution challenge: towards a circular economy, Green Chem. 22 (2020) 6310–6322. https://doi.org/10.1039/D0GC02630A.

[72] A. Reznichenko, A. Harlin, Next generation of polyolefin plastics: improving sustainability with existing and novel feedstock base, SN Appl. Sci. 4 (2022) 108. https://doi.org/10.1007/s42452-022-04991-4.

[73] Z. Zhao, J. Jiang, F. Wang, An economic analysis of twenty light olefin production pathways, Journal of Energy Chemistry. 56 (2021) 193–202. https://doi.org/10.1016/j.jechem.2020.04.021.

[74] Z. Gholami, F. Gholami, Z. Tišler, M. Tomas, M. Vakili, A Review on Production of Light Olefins via Fluid Catalytic Cracking, Energies. 14 (2021) 1089. https://doi.org/10.3390/en14041089.

[75] I. Amghizar, L.A. Vandewalle, K.M. Van Geem, G.B. Marin, New Trends in Olefin Production, Engineering. 3 (2017) 171–178. https://doi.org/10.1016/J.ENG.2017.02.006.

[76] I. Amghizar, J.N. Dedeyne, D.J. Brown, G.B. Marin, K.M. Van Geem, Sustainable innovations in steam cracking: CO_2 neutral olefin production, React. Chem. Eng. 5 (2020) 239–257. https://doi.org/10.1039/C9RE00398C.

[77] V. Zacharopoulou, A. Lemonidou, Olefins from Biomass Intermediates: A Review, Catalysts. 8 (2017) 2. https://doi.org/10.3390/catal8010002.

[78] T. Ren, M. Patel, K. Blok, Olefins from conventional and heavy feedstocks: Energy use in steam cracking and alternative processes, Energy. 31 (2006) 425–451. https://doi.org/10.1016/j.energy.2005.04.001.

[79] Y. Chan, L. Petithuguenin, T. Fleiter, A. Herbst, M. Arens, P. Stevenson, Part 1: Technology Analysis, (n.d.) 124.

[80] European Commission. Joint Research Centre., Best Available Techniques (BAT) reference document for the production of large volume organic chemicals., Publications Office, LU, 2017. https://data.europa.eu/doi/10.2760/77304 (accessed May 23, 2022).

[81] V.P. Haribal, Y. Chen, L. Neal, F. Li, Intensification of Ethylene Production from Naphtha via a Redox Oxy-Cracking Scheme: Process Simulations and Analysis, Engineering. 4 (2018) 714–721. https://doi.org/10.1016/j.eng.2018.08.001.

[82] M.I. Bayazitov, A.V. Rubtsov, P.A. Kulakov, R.M. Bayazitov, Identification of damages zones of transfer line exchanger based on modeling, J. Phys.: Conf. Ser. 1399 (2019) 055071. https://doi.org/10.1088/1742-6596/1399/5/055071.

[83] Z. Gholami, F. Gholami, Z. Tišler, M. Vakili, A Review on the Production of Light Olefins Using Steam Cracking of Hydrocarbons, Energies. 14 (2021) 8190. https://doi.org/10.3390/en14238190.

[84] Y. Gao, L. Neal, D. Ding, W. Wu, C. Baroi, A.M. Gaffney, F. Li, Recent Advances in Intensified Ethylene Production—A Review, ACS Catal. 9 (2019) 8592–8621. https://doi.org/10.1021/acscatal.9b02922.

[85] C.C.N. Oliveira, P.R.R. Rochedo, R. Bhardwaj, E. Worrell, A. Szklo, Bio-ethylene from sugarcane as a competitiveness strategy for the Brazilian chemical industry, Biofuels, Bioprod. Bioref. 14 (2020) 286–300. https://doi.org/10.1002/bbb.2069.

[86] Z. Zhao, K. Chong, J. Jiang, K. Wilson, X. Zhang, F. Wang, Low-carbon roadmap of chemical production: A case study of ethylene in China, Renewable and Sustainable Energy Reviews. 97 (2018) 580–591. https://doi.org/10.1016/j.rser.2018.08.008.

[87] M.G. Lobo, E. Dorta, Utilization and Management of Horticultural Waste, in: Postharvest Technology of Perishable Horticultural Commodities, Elsevier, 2019: pp. 639–666. https://doi.org/10.1016/B978-0-12-813276-0.00019-5.

[88] D. Fan, D.-J. Dai, H.-S. Wu, Ethylene Formation by Catalytic Dehydration of Ethanol with Industrial Considerations, Materials. 6 (2012) 101–115. https://doi.org/10.3390/ma6010101.

[89] A. Mohsenzadeh, A. Zamani, M.J. Taherzadeh, Bioethylene Production from Ethanol: A Review and Techno-economical Evaluation, ChemBioEng Reviews. 4 (2017) 75–91. https://doi.org/10.1002/cben.201600025.

[90] A.Z. Turan, Ö. Ataç, O.A. Kurucu, A. Ersöz, A. Sarıoğlan, H. Okutan, Kinetic modeling of Fischer–Tropsch-to-olefins process via advanced optimization, Int. J. Chem. Kinet. 54 (2022) 3–15. https://doi.org/10.1002/kin.21536.

[91] Y. Liu, H. Kamata, H. Ohara, Y. Izumi, D.S.W. Ong, J. Chang, C.K. Poh, L. Chen, A. Borgna, Low-Olefin Production Process Based on Fischer–Tropsch Synthesis: Process Synthesis, Optimization, and Techno-Economic Analysis, Ind. Eng. Chem. Res. 59 (2020) 8728–8739. https://doi.org/10.1021/acs.iecr.0c00542.

[92] M.E. Dry, High quality diesel via the Fischer-Tropsch process - a review, J. Chem. Technol. Biotechnol. 77 (2002) 43–50. https://doi.org/10.1002/jctb.527.

[93] X. Zhou, J. Ji, D. Wang, X. Duan, G. Qian, D. Chen, X. Zhou, Hierarchical structured α-Al $_2$ O $_3$ supported S-promoted Fe catalysts for direct conversion of syngas to lower olefins, Chem. Commun. 51 (2015) 8853–8856. https://doi.org/10.1039/C5CC00786K.

[94] A.K. Rausch, L. Schubert, R. Henkel, E. van Steen, M. Claeys, F. Roessner, Enhanced olefin production in Fischer–Tropsch synthesis using ammonia containing synthesis gas feeds, Catalysis Today. 275 (2016) 94–99. https://doi.org/10.1016/j.cattod.2016.02.002.

[95] Z. Gholami, F. Gholami, Z. Tišler, J. Hubáček, M. Tomas, M. Bačiak, M. Vakili, Production of Light Olefins via Fischer-Tropsch Process Using Iron-Based Catalysts: A Review, Catalysts. 12 (2022) 174. https://doi.org/10.3390/catal12020174.

[96] B.H. Davis, B.B. Breman, A.P. Steynberg, M.E. Dry, Fischer-Tropsch Reactors, in: A.P. Steynberg, M.E. Dry (Eds.), Fischer-Tropsch Technology, Elsevier, 2004: pp. 64–195. https://doi.org/10.1016/S0167-2991(04)80459-2.

[97] D.S. Lima, O.W. Perez-Lopez, Oxidative coupling of methane to light olefins using waste eggshell as catalyst, Inorganic Chemistry Communications. 116 (2020) 107928. https://doi.org/10.1016/j.inoche.2020.107928.

[98] G.J. Hutchings, M.S. Scurrell, J.R. Woodhouse, Oxidative coupling of methane using oxide catalysts, Chem. Soc. Rev. 18 (1989) 251. https://doi.org/10.1039/cs9891800251.

[99] R. Alkathiri, A. Alshamrani, I. Wazeer, M. Boumaza, M.K. Hadj-Kali, Optimization of the Oxidative Coupling of Methane Process for Ethylene Production, Processes. 10 (2022) 1085. https://doi.org/10.3390/pr10061085.

[100] P. Wang, X. Zhang, G. Zhao, Y. Liu, Y. Lu, Oxidative coupling of methane: MO x - modified (M = Ti, Mg, Ga, Zr) Mn 2 O 3 -Na 2 WO 4 /SiO 2 catalysts and effect of MO x modification, Chinese Journal of Catalysis. 39 (2018) 1395–1402. https://doi.org/10.1016/S1872-2067(18)63076-1.

[101] C. Karakaya, H. Zhu, C. Loebick, J.G. Weissman, R.J. Kee, A detailed reaction mechanism for oxidative coupling of methane over Mn/Na2WO4/SiO2 catalyst for non-isothermal conditions, Catalysis Today. 312 (2018) 10–22. https://doi.org/10.1016/j.cattod.2018.02.023.

[102] T. Wang, J. Wang, MULTIPHASE FLOW REACTORS FOR METHANOL AND DIMETHYL ETHER PRODUCTION, in: Y. Cheng, F. Wei, Y. Jin (Eds.), Multiphase Reactor Engineering for Clean and Low-Carbon Energy Applications, John Wiley & Sons, Inc., Hoboken, NJ, USA, 2017: pp. 189–218. https://doi.org/10.1002/9781119251101.ch6.

[103] A.C. Dimian, C.S. Bildea, Energy efficient methanol-to-olefins process, Chemical Engineering Research and Design. 131 (2018) 41–54. https://doi.org/10.1016/j.cherd.2017.11.009.

[104] A.L. Andrady, Plastics and Environmental Sustainability: Andrady/Plastics and Environmental Sustainability, John Wiley & Sons, Inc, Hoboken, NJ, 2015. https://doi.org/10.1002/9781119009405.

[105] Y. Khojasteh-Salkuyeh, O. Ashrafi, E. Mostafavi, P. Navarri, CO2 utilization for methanol production; Part I: Process design and life cycle GHG assessment of different pathways, Journal of CO2 Utilization. 50 (2021) 101608. https://doi.org/10.1016/j.jcou.2021.101608.

[106] A.E. Khamlichi, N. Thybaud, Chemical conversion of CO2: overview, quantification of energy and environmental benefits and economic evaluation of three chemical routes; Report of the French Environment and Enrgy Management Agency (ADEME), France, 2014.

[107] Y. Khojasteh Salkuyeh, T.A. Adams II, Co-Production of Olefins, Fuels, and Electricity from Conventional Pipeline Gas and Shale Gas with Near-Zero CO2 Emissions. Part I: Process Development and Technical Performance, Energies. 8 (2015) 3739–3761.

[108] Y. Khojasteh Salkuyeh, T.A. Adams II, Co-Production of Olefins, Fuels, and Electricity from Conventional Pipeline Gas and Shale Gas with Near-Zero CO2 Emissions. Part II: Economic Performance, Energies. 8 (2015) 3762–3774.

[109] V. Dieterich, A. Buttler, A. Hanel, H. Spliethoff, S. Fendt, Power-to-liquid via synthesis of methanol, DME or Fischer–Tropsch-fuels: a review, Energy Environ. Sci. 13 (2020) 3207–3252. https://doi.org/10.1039/D0EE01187H.

[110] F.J. Keil, Methanol-to-hydrocarbons: process technology, Microporous and Mesoporous Materials. 29 (1999) 49–66. https://doi.org/10.1016/S1387-1811(98)00320-5.

[111] M.R. Gogate, Methanol-to-olefins process technology: current status and future prospects, Null. 37 (2019) 559–565. https://doi.org/10.1080/10916466.2018.1555589.

[112] S. Wilson, P. Barger, The characteristics of SAPO-34 which influence the conversion of methanol to light olefins, Microporous and Mesoporous Materials. 29 (1999) 117–126. https://doi.org/10.1016/S1387-1811(98)00325-4.

[113] Intraec, Ethylene production from methanol, Ethylene E91A Advanced Cost Analysis, Intratec Solutions, LLC, 2019. https://www.intratec.us/analysis/ethylene-e91a.

[114] A.C. Dimian, C.S. Bildea, Energy efficient methanol-to-olefins process, Chemical Engineering Research and Design. 131 (2018) 41–54. https://doi.org/10.1016/j.cherd.2017.11.009.

[115] Y. Khojasteh-Salkuyeh, A. Elkamel, J. Thé, M. Fowler, Development and techno-economic analysis of an integrated petroleum coke, biomass, and natural gas polygeneration process, Energy. 113 (2016) 861–874.

[116] INTEGRATION Software; https://www.nrcan.gc.ca/energy-efficiency/industrial-systems-optimization/process-integration-pinch-analys/products-services/integration-software/5529, (n.d.).

[117] F.-O. Mähling, D. Littmann, A. Daiss, Method for the continuous production of ethylene homo- and ethylene co-polymers, WO2001085807A1, 2001. https://patents.google.com/patent/WO2001085807A1/en (accessed June 1, 2022).

[118] Aspen Polymers Plus Examples and Applications, (2006). http://www.aspentech.com.

[119] M. Häfele, A. Kienle, M. Boll, C.-U. Schmidt, M. Schwibach, Dynamic simulation of a tubular reactor for the production of low-density polyethylene using adaptive method of lines, Journal of Computational and Applied Mathematics. 183 (2005) 288–300. https://doi.org/10.1016/j.cam.2004.12.033.

[120] F.Z. Yao, A. Lohi, S.R. Upreti, R. Dhib, Modeling, Simulation and Optimal Control of Ethylene Polymerization in Non-Isothermal, High-Pressure Tubular Reactors, International

Journal of Chemical Reactor Engineering. 2 (2004). https://doi.org/10.2202/1542-6580.1152.

[121] R.M. Patel, Multilayer Flexible Packaging, Elsevier, 2016. https://doi.org/10.1016/C2014-0-02918-8.

[122] Mitsui Chemicals, CX technology for HDPE project, (2020). https://jp.mitsuichemicals.com/en/techno/license/pdf/cx_process.pdf?201022.

[123] Y. Guerrieri, K. Valverde, G.M. Nunes Costa, M. Embiruu, A Survey of Equations of State for Polymers, in: A. De Souza Gomes (Ed.), Polymerization, InTech, 2012. https://doi.org/10.5772/48391.

[124] C. Zhang, Z. Shao, X. Chen, Z. Yao, X. Gu, L.T. Biegler, Kinetic parameter estimation of HDPE slurry process from molecular weight distribution: Estimability analysis and multistep methodology, AIChE J. 60 (2014) 3442–3459. https://doi.org/10.1002/aic.14527.

[125] S. Ronca, Polyethylene, in: Brydson's Plastics Materials, Elsevier, 2017: pp. 247–278. https://doi.org/10.1016/B978-0-323-35824-8.00010-4.

[126] C.P. Bokis, S. Ramanathan, J. Franjione, A. Buchelli, M.L. Call, A.L. Brown, Physical Properties, Reactor Modeling, and Polymerization Kinetics in the Low-Density Polyethylene Tubular Reactor Process, Ind. Eng. Chem. Res. 41 (2002) 1017–1030. https://doi.org/10.1021/ie010308e.

[127] M. Salami-Kalajahi, V. Haddadi-Asl, M. Najafi, S.M. Ghafelebashi Zarand, Investigation of Ethylene Polymerization Kinetics over Ziegler-Natta Catalysts: Employing Moment Equation Modeling to Study the Effect of Different Active Centers on Homopolymerization Kinetics, E-Polymers. 8 (2008). https://doi.org/10.1515/epoly.2008.8.1.29.

[128] F. Gemoets, M. Zhang, T.W. Karjala, B.W.S. Kolthammer, Kinetic Study of Ethylene Homopolymerization in Slurry Using a Ziegler-Natta.pdf, Macromolecular Reaction Engineering. 4 (2010) 109–122.

[129] K.B. McAuley, J.F. MacCregor, A.E. Hamielec, A kinetic model for industrial gas-phase ethylene copolymerization, AICHE. 36 (1990).

[130] Y.V. Kissin, Main Kinetic Features of Ethylene Polymerization Reactions with Heterogeneous Ziegler-Natta Catalysts in the Light of Multi-Center Reaction Mechanism, in: R. Blom, A. Follestad, E. Rytter, M. Tilset, M. Ystenes (Eds.), Organometallic Catalysts and Olefin Polymerization, Springer Berlin Heidelberg, Berlin, Heidelberg, 2001: pp. 217–228. https://doi.org/10.1007/978-3-642-59465-6_18.

[131] Provincial and Territorial Energy Profiles, (2022). https://www.cer-rec.gc.ca/en/data-analysis/energy-markets/provincial-territorial-energy-profiles/index.html (accessed June 2, 2022).

[132] Comparing power generation options and electricity mixes, CIRAIG, 2014. https://ciraig.org/index.php/lca-study/comparing-power-generation-options-and-electricity-mixes/ (accessed June 2, 2022).

[133] J.C. Bare, P. Hofstetter, D.W. Pennington, H.A.U. de Haes, Midpoints versus endpoints: The sacrifices and benefits, Int. J. LCA. 5 (2000) 319. https://doi.org/10.1007/BF02978665.

[134] M.A.J. Huijbregts, Z.J.N. Steinmann, P.M.F. Elshout, G. Stam, F. Verones, M. Vieira, M. Zijp, A. Hollander, R. van Zelm, ReCiPe2016: a harmonised life cycle impact assessment method at midpoint and endpoint level, Int J Life Cycle Assess. 22 (2017) 138–147. https://doi.org/10.1007/s11367-016-1246-y.

[135] J.C. Bare, Traci.: The Tool for the Reduction and Assessment of Chemical and Other Environmental Impacts, Journal of Industrial Ecology. 6 (2002) 49–78. https://doi.org/10.1162/108819802766269539.

[136] R. Arvidsson, M. Svanström, S. Harvey, B.A. Sandén, Life-cycle impact assessment methods for physical energy scarcity: considerations and suggestions, Int J Life Cycle Assess. 26 (2021) 2339–2354. https://doi.org/10.1007/s11367-021-02004-x.